

Tensor networks for non-invertible symmetries in 3+1d and beyond

Pranay Gorantla¹, Shu-Heng Shao^{2,3}, Nathanan Tantivasadakarn⁴

¹*Kadanoff Center for Theoretical Physics & Enrico Fermi Institute, University of Chicago*

²*Yang Institute for Theoretical Physics, Stony Brook University*

³*Center for Theoretical Physics, Massachusetts Institute of Technology*

⁴*Walter Burke Institute for Theoretical Physics and Department of Physics, California Institute of Technology*

Abstract

Tensor networks provide a natural language for non-invertible symmetries in general Hamiltonian lattice models. We use ZX-diagrams, which are tensor network presentations of quantum circuits, to define a non-invertible operator implementing the Wegner duality in 3+1d lattice \mathbb{Z}_2 gauge theory. The non-invertible algebra, which mixes with lattice translations, can be efficiently computed using ZX-calculus. We further deform the \mathbb{Z}_2 gauge theory while preserving the duality and find a model with nine exactly degenerate ground states on a torus, consistent with the Lieb-Schultz-Mattis-type constraint imposed by the symmetry. Finally, we provide a ZX-diagram presentation of the non-invertible duality operators (including non-invertible parity/reflection symmetries) of generalized Ising models based on graphs, encompassing the 1+1d Ising model, the three-spin Ising model, the Ashkin-Teller model, and the 2+1d plaquette Ising model. The mixing (or lack thereof) with spatial symmetries is understood from a unifying perspective based on graph theory.

Contents

1	Introduction	2
2	Review of ZX-calculus	5
3	Non-invertible Kramers-Wannier operator in 1+1d	9
3.1	Non-invertible Kramers-Wannier duality operator	10
3.2	Action on operators	12
3.3	Operator algebra	14
3.4	Action on states	16
4	Review of 3+1d lattice \mathbb{Z}_2 gauge theory	17
4.1	Topological versus non-topological 1-form global symmetries	18
4.2	Defects for the 1-form symmetry	19
4.3	Gauging the 1-form symmetry and the Wegner duality	20
5	Non-invertible Wegner operator in 3+1d	22
5.1	Non-invertible duality symmetry as a tensor network operator	24
5.2	Action on operators	25
5.3	Operator algebra and the condensation operator	27
5.4	Lattice symmetries	30
5.5	Action on the toric code ground states	31
5.6	LSM-type constraint and duality-preserving deformations	32
6	Non-invertible symmetries based on graphs	34
6.1	Hamiltonian of the generalized transverse-field Ising model	35
6.2	Spatial symmetries from preserving automorphisms	36
6.3	Non-invertible duality operators from reversing automorphisms	37
6.4	Action on operators	38
6.5	Operator algebra	38
6.6	Examples	41
6.6.1	1+1d Ising model	41
6.6.2	3+1d lattice \mathbb{Z}_2 gauge theory	42

6.6.3	1+1d Ashkin-Teller model	43
6.6.4	1+1d three-spin Ising model	44
6.6.5	2+1d plaquette Ising model	45
6.6.6	Tensor product models	46
6.6.7	On mixing with spatial symmetries	48
7	Discussions and Outlook	49
A	ZX-calculus for the duality and condensation operators	50
A.1	Condensation operator	51
A.2	Duality operator	51
A.3	Action of D on the states	55
A.4	Ground states of 3+1d toric code	56
B	Higher quantum symmetry	58

1 Introduction

The symmetry principle in theoretical physics has been generalized in many different directions in recent years. In particular, it has become increasingly clear that symmetries in quantum system need not be invertible. These *non-invertible symmetries* are not described by group theory, and go beyond the paradigm set by Wigner’s theorem. Nonetheless, they exist ubiquitously in many familiar quantum field theories and lattice models, leading to new conservation laws and selection rules. See [1–8] for reviews.

The simplest example of non-invertible symmetries is the Kramers-Wannier (KW) symmetry of the 1+1d Ising lattice model [9–13]. In particular, it has been realized recently that in the quantum Hamiltonian Ising lattice model, the operator algebra of this non-invertible symmetry mixes with the lattice translation [14, 15].¹ This symmetry implies a Lieb-Schultz-Mattis (LSM) type constraint [18, 15], forbidding a trivially gapped phase. See, for examples, [19–36] for recent discussions of non-invertible symmetries in 1+1d lattice systems, and [37–46] for 2+1d examples.

The most natural generalization of the Kramers-Wannier duality in 1+1d is the Wegner duality in 3+1d lattice \mathbb{Z}_2 gauge theory [47].² While the Kramers-Wannier duality exchanges the broken

¹On the other hand, a general fusion category can be realized with no mixing with the lattice translation on an anyonic chain [16, 17], which generally does not have a tensor product Hilbert space.

²Note that in 2+1d, the Ising lattice model is not self-dual under gauging; rather, it is mapped to the lattice \mathbb{Z}_2 gauge theory. The corresponding non-invertible symmetry in \mathbb{Z}_2 gauge theory coupled to Ising matter is constructed in [44] and generalized in Section 6.6.6. This is related to the fact that gauging a $\mathbb{Z}_2^{(q)}$ symmetry in $(d+1)$ d returns a dual $\mathbb{Z}_2^{(d-q-1)}$ symmetry [48, 49]. (The superscript (q) denotes the form degree of a q -form global symmetry.) Hence,

and unbroken phases of an ordinary $\mathbb{Z}_2^{(0)}$ symmetry, the Wegner duality exchanges those of a $\mathbb{Z}_2^{(1)}$ one-form global symmetry. At the self-dual point, the Wegner duality leads to a non-invertible symmetry. The topological defect associated with this symmetry was constructed in the Euclidean lattice gauge theory in [50], and its continuum counterpart was found in [51, 52].

In this work, we derive the corresponding non-invertible duality *operator* in the quantum Hamiltonian lattice \mathbb{Z}_2 gauge theory in 3+1d on a tensor product Hilbert space, generalizing the KW operator of the 1+1d transverse-field Ising model.

To this end, we use the *tensor network* formalism [53, 54] to present these non-invertible operators in general dimensions. On the lattice, tensor networks are a natural tool to describe non-unitary operators. In particular, non-invertible symmetries in one spatial dimension have been recently studied on the lattice using a class of tensor networks called matrix product operators [55–64, 15]. In this work, we use a particular formulation of tensor networks called *ZX-calculus* [65, 66] (see [67] for a review). ZX-calculus is a graphical language to reason about linear maps between qubits. It is a concrete realization of a more abstract program of diagrammatic reasoning in quantum physics [68, 69]. It has roots in quantum foundations, but has recently gained popularity in practical applications in quantum information ranging from optimizing quantum circuits [70–72] to concepts in quantum error correction and fault-tolerant quantum computation [73–79].

The central object of ZX-calculus is a *ZX-diagram*. It is a string diagram/tensor network representation of a quantum circuit, or more generally, a linear map between qubits. One of the most important features of a ZX-diagram is that it can be deformed arbitrarily, while maintaining the connectivity, without changing the linear map it represents. In other words, *only topology of the diagram matters*. Furthermore, a ZX-diagram can be modified to another topologically-inequivalent diagram using a simple (and finite) set of local moves known as *rewrite rules*. Much of the power of ZX-calculus derives from the *completeness* of these rewrite rules, i.e., any reasoning about linear maps between qubits can be done entirely graphically using a finite sequence of rewrite rules. This is in contrast to the most general formulation of tensor networks, where a general product of tensors increases the bond dimension, and does not have an obvious algorithm to simplify the tensors (especially in the case of high connectivity).

The Kramers-Wannier duality operator in 1+1d and the Wegner duality operator in 3+1d admit a simple presentation as ZX-diagrams: first, we construct the duality *maps* represented by the ZX-diagrams shown in Figure 1, and then, we compose them with *half-translation maps* (not shown in the figure). In both cases, the duality map takes the original lattice to the dual lattice, and the half-translation map takes it back to the original lattice. In the end, we get an *operator* on the original Hilbert space.

Using ZX-calculus, we derive the non-invertible operator algebras for the 1+1d KW duality symmetry and that for the 3+1d Wegner duality symmetry in a uniform manner. In particular, we find that the algebra of the Wegner duality operator D involves a lattice translation in the $(1, 1, 1)$ direction, generalizing the 1+1d observation in [18, 15]. See Table 1. The non-invertible operator D

the dual symmetry can be isomorphic to the original one only if $q = 0, d = 1$ and $q = 1, d = 3$.

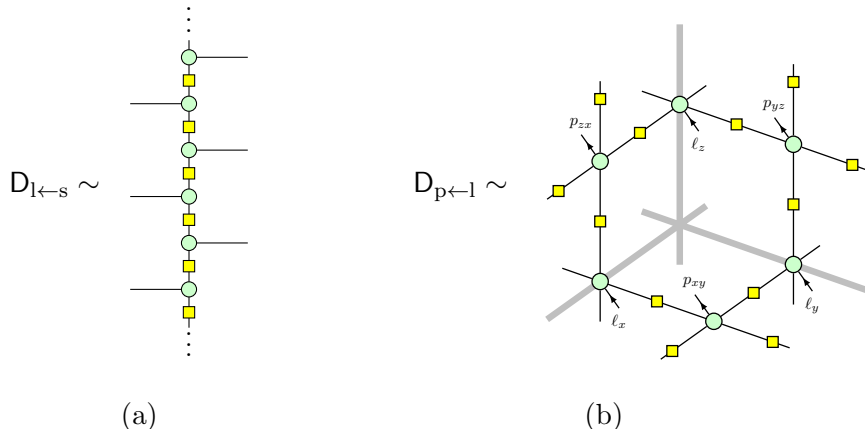


Figure 1: The tensor network representations, or the ZX-diagrams, of (a) the Kramers-Wannier duality map in 1+1d and (b) the Wegner duality map in 3+1d. In (a), time flows from left to right, so the input legs are on the sites of the periodic chain and the output legs are on the links. In (b), the flow of time is indicated by the arrows, so the input legs are on the links (thick gray lines) of the periodic cubic lattice and the output legs are on the plaquettes. (We show only the part of the diagram in a unit cell; the full diagram is obtained by repeating and gluing this diagram periodically in the three spatial directions.)

exchanges the product state with the 3+1d toric code ground state. We also define a condensation operator C on the lattice, which creates a 3+1d toric code ground state from a product state.

We further discuss a deformation of the lattice \mathbb{Z}_2 gauge theory while preserving the non-invertible Wegner duality symmetry. This is a direct generalization of the deformation of the 1+1d Ising model in [80]. We argue for an LSM-type constraint for the non-invertible symmetry, which implies that the deformed model cannot be trivially gapped.

Finally, our tensor network presentation of the non-invertible symmetry can be readily extended to generalized transverse-field Ising models (TFIMs) based on arbitrary bipartite graphs. We present the condition under which such a model has a non-invertible duality symmetry, and derive a condition for when the non-invertible operator algebra mixes with the spatial symmetry. We then discuss several examples of non-invertible symmetries in this unifying presentation. In some examples, we find a non-invertible parity (or reflection) symmetry.

The rest of this paper is organized as follows. Section 2 reviews some of the essential elements of the ZX-calculus. Section 3 demonstrates the utility of tensor network representation and ZX-calculus in constructing and analyzing the 1+1d Kramers-Wannier duality operator. Section 4 gives a brief review of the 3+1d lattice \mathbb{Z}_2 gauge theory, gauging the \mathbb{Z}_2 1-form symmetry, and Wegner duality. Section 5 gives the explicit tensor network representation of the 3+1d Wegner duality operator and the derivation of its operator algebra using ZX-calculus. Section 6 presents the tensor network representation of the non-invertible duality operator and its algebra in the generalized TFIM based on an arbitrary bipartite graph. Section 7 concludes with a discussion of the results

	1+1d	3+1d
Continuum	$\mathcal{D}^2 = 1 + \eta$	$\mathcal{D}(M)^2 = \frac{1}{ H^0(M, \mathbb{Z}_2) } \sum_{\Sigma \in H_2(M, \mathbb{Z}_2)} \eta(\Sigma) =: \mathcal{C}(M)$
Lattice	$\mathbf{D}^2 = (1 + \eta)T$	$\mathbf{D}^2 = \frac{1}{2^V} T_{1,1,1} \sum_{\hat{\Sigma}} \eta(\hat{\Sigma}) =: \mathbf{C}T_{1,1,1}$

Table 1: The operator algebras of the Kramers-Wannier duality operator in 1+1d and the Wegner duality operator in 3+1d with themselves in the continuum and on the lattice. Here, η is the ordinary \mathbb{Z}_2 symmetry operator in 1+1d, while $\eta(\Sigma)$ is a 1-form symmetry operator on a 2-cycle Σ in 3+1d. Finally, M is a spatial 3-manifold, T is the generator of spatial translation in 1+1d, and $T_{1,1,1}$ is the generator of spatial translation in the (1, 1, 1) direction in 3+1d.

and potential future directions. Appendix A gives the details of several derivations involving the Wegner duality operator and the condensation operator using ZX-calculus. And finally, Appendix B gives the tensor network representation of the higher quantum symmetry operators associated with higher-gauging the \mathbb{Z}_2 1-form symmetry on the lattice.

2 Review of ZX-calculus

A ZX-diagram is a graphical representation of a linear map of qubits.³ It is built out of the following generators.

1. Z-spider: $n \text{ : } \begin{array}{c} \text{---} \\ \text{---} \end{array} \begin{array}{c} \text{---} \\ \text{---} \end{array} \text{ : } m := |0\rangle^{\otimes m} \langle 0|^{\otimes n} + e^{i\alpha} |1\rangle^{\otimes m} \langle 1|^{\otimes n}$.
2. X-spider: $n \text{ : } \begin{array}{c} \text{---} \\ \text{---} \end{array} \begin{array}{c} \text{---} \\ \text{---} \end{array} \text{ : } m := |+\rangle^{\otimes m} \langle +|^{\otimes n} + e^{i\alpha} |-\rangle^{\otimes m} \langle -|^{\otimes n}$.
3. Hadamard, H: $\text{---} \begin{array}{c} \text{---} \\ \text{---} \end{array} \text{---} := \frac{1}{\sqrt{2}} (|0\rangle \langle 0| + |0\rangle \langle 1| + |1\rangle \langle 0| - |1\rangle \langle 1|)$.
4. Identity: $\text{---} := |0\rangle \langle 0| + |1\rangle \langle 1|$.
5. SWAP: $\text{---} \text{---} := |00\rangle \langle 00| + |01\rangle \langle 10| + |10\rangle \langle 01| + |11\rangle \langle 11|$.
6. A Bell pair (ket): $\text{---} \text{---} := |00\rangle + |11\rangle$.
7. A Bell pair (bra): $\text{---} \text{---} := \langle 00| + \langle 11|$.

Here, $n, m \in \mathbb{N} = \{0, 1, 2, \dots\}$ and $\alpha \sim \alpha + 2\pi$. It is customary to omit the phase α inside the Z/X-spiders if $\alpha = 0$. The following are elementary examples of ZX-diagrams of some familiar states and operators.

1. Eigenstates of Pauli Z: $\text{---} \begin{array}{c} \text{---} \\ \text{---} \end{array} \text{---} = \sqrt{2}|0\rangle$ and $\text{---} \begin{array}{c} \text{---} \\ \text{---} \end{array} \text{---} = \sqrt{2}|1\rangle$.

³This includes states (or kets), which are linear maps with domain \mathbb{C} , and their adjoints (or bras), which are linear maps with codomain \mathbb{C} .

2. Eigenstates of Pauli X : $\circ\text{---} = \sqrt{2}|+\rangle$ and $\pi\text{---} = \sqrt{2}|-\rangle$.
3. A Bell pair (ket): $\curvearrowright = \curvearrowleft = \frown = |00\rangle + |11\rangle$.
4. GHZ state: $\curvearrowleft = |000\rangle + |111\rangle$.⁴
5. Pauli Z : $\text{---}\pi\text{---} = |0\rangle\langle 0| - |1\rangle\langle 1|$.
6. Pauli X : $\text{---}\pi\text{---} = |+\rangle\langle +| - |-\rangle\langle -|$.
7. Controlled-NOT gate, $\text{CNOT}_{i,j}$: $\sqrt{2} \begin{array}{c} i \text{---} \circ \text{---} i \\ | \\ j \text{---} \pi \text{---} j \end{array} = |0\rangle\langle 0|_i \otimes I_j + |1\rangle\langle 1|_i \otimes X_j$.
8. Controlled- Z gate, $\text{CZ}_{i,j}$: $\sqrt{2} \begin{array}{c} i \text{---} \circ \text{---} i \\ | \\ j \text{---} \square \text{---} j \\ | \\ j \text{---} \circ \text{---} j \end{array} = \frac{1}{2}(1 + Z_i + Z_j - Z_i Z_j)$.

Note that the ZX-diagrams of CNOT and CZ gates involve more than one generator. Indeed, one can build more general maps by combining ZX-diagrams as follows: let D_1 and D_2 be two diagrams with associated matrices denoted as $[D_1]$ and $[D_2]$, respectively.

1. The diagram associated with the *tensor product* $[D_1] \otimes [D_2]$ is obtained by placing them together. For example,

$$\begin{array}{c} \circ \text{---} i \\ | \\ \pi \text{---} j \end{array} = (\sqrt{2})^2 |0\rangle_i \otimes |1\rangle_j . \quad (2.1)$$

2. The diagram associated with the *product* or *composition* $[D_2][D_1]$, provided it is well-defined, is obtained by joining the outputs of D_1 to the inputs of D_2 .⁵ For example,

$$\text{---}\pi\text{---}\pi\text{---} = XZ = -iY . \quad (2.2)$$

In fact, any map of qubits can be represented as a ZX-diagram built out of the above generators using the above composition rules. This property is known as *universality*.

Given two ZX-diagrams, one natural question is if they represent the same map. There is a set of rewrite rules, known as the ZX-calculus, that allows one to transform a given diagram to obtain another diagram representing the same map. Some of them are listed below (the full set can be found in [67] for instance).

(SF) Spider fusion: $\begin{array}{c} n \text{---} \circ \text{---} m \\ | \\ k \text{---} \circ \text{---} l \end{array} = n+k \text{---} \circ \text{---} m+l$ and similarly for the X-spiders.

(I) Identity removal: $\text{---}\circ\text{---} = \text{---}\pi\text{---} = \text{---}$.

⁴Here, a helpful mnemonic is that the **GHZ** state is constructed from the **Green Z**-spider.

⁵Unless otherwise specified, we place the inputs (outputs) on the left (right) so that “time” flows from left to right. Where this is not possible—for example, in higher dimensional systems—we use ingoing (outgoing) arrows to represent the inputs (outputs).

diagrams on the left and right is a manifestation of the slogan “only topology matters.” This is why there is no ambiguity in the definition of the diagram in the middle.

These rules are so powerful that one can prove entirely graphically whatever one can prove using matrices, i.e., if D_1 and D_2 represent the diagrams of two matrices, denoted as $[D_1]$ and $[D_2]$, then $[D_1] = [D_2]$ if and only if there is a finite sequence of rules that transform D_1 to D_2 . The “if” direction is known as *soundness* and the “only if” direction is known as *completeness*.⁶

In many cases, a diagram contains several copies of a smaller diagram. In such cases, it is convenient to use the annotated !-box (read as “bang box”). For example,

(2.4)

Here, the part of the diagram inside the annotated !-box (the blue box) is repeated three times, and each copy, labelled by $i = 1, 2, 3$, is connected to the part of the diagram outside the annotated !-box in the same way.

It is also convenient to define a “periodic” version of the annotated !-box. For example,

(2.5)

It is very similar to the annotated !-box except that the wires that end on the dashed blue lines are glued together in a periodic way. Note that when there are no wires that end on the dashed lines, there is no difference between the two boxes, so we will use the periodic version only when there are wires that end on the dashed lines. Moreover, in what follows, it is always understood that i labels the sites of a periodic 1d chain with L sites, so we omit the annotation “ $i = 1, \dots, L$ ” above the box.

Lastly, for completeness, we mention the following. Given a ZX-diagram D representing a map $[D]$, we can obtain the ZX-diagram of

1. its *conjugate* $[D]^*$ by flipping the signs of all the phases in the spiders in D ,

⁶One has to add more rules to the list above so that the ZX-calculus is complete. We do not go into the details here and point interested readers to [67].

2. its *transpose* $[D]^\top$ by flipping the diagram about the vertical axis (or reversing the flow of time), and
3. its *adjoint* $[D]^\dagger$ by doing both.

3 Non-invertible Kramers-Wannier operator in 1+1d

In this section, we review the non-invertible Kramers-Wannier operator of the critical Ising lattice model in 1+1d using the language of ZX-calculus.

Consider a periodic chain of L sites, labelled by $i = 1, \dots, L$, with a qubit at each site, i.e., $\mathcal{H}_i \cong \mathbb{C}^2$. The total Hilbert space is the tensor product $\mathcal{H} = \bigotimes_i \mathcal{H}_i$. The Pauli operators acting on the site i are labelled as Z_i and X_i . An eigenstate of the Z_i 's is denoted as $|\{m_i\}\rangle := \bigotimes_i |m_i\rangle$ with $m_i \in \{0, 1\}$. The corresponding ZX-diagram is

$$|\{m_i\}\rangle = \frac{1}{2^{L/2}} \begin{array}{c} \vdots \\ \textcircled{m_{i-1}\pi} \\ \textcircled{m_i\pi} \\ \textcircled{m_{i+1}\pi} \\ \vdots \end{array} = \frac{1}{2^{L/2}} \boxed{\textcircled{m_i\pi} - i}, \quad (3.1)$$

Similarly, an eigenstate of the X_i 's is denoted as $|\{(-)^{m_i}\}\rangle := \bigotimes_i |(-)^{m_i}\rangle$ with $m_i \in \{0, 1\}$. The corresponding ZX-diagram is

$$|\{(-)^{m_i}\}\rangle = \frac{1}{2^{L/2}} \begin{array}{c} \vdots \\ \textcircled{m_{i-1}\pi} \\ \textcircled{m_i\pi} \\ \textcircled{m_{i+1}\pi} \\ \vdots \end{array} = \frac{1}{2^{L/2}} \boxed{\textcircled{m_i\pi} - i}. \quad (3.2)$$

While most of our discussions below concern with only the operators on the Hilbert space \mathcal{H} , it is useful to have in mind a specific example of a Hamiltonian. We start with the Hamiltonian of the 1+1d transverse-field Ising model

$$H = -J \sum_{i=1}^L Z_i Z_{i+1} - h \sum_{i=1}^L X_i, \quad (3.3)$$

but our discussion applies to more general Hamiltonians with the same symmetries of interest. (See (3.32) for an example.) The Ising Hamiltonian is translationally invariant, i.e., H commutes with

the generator of translation

$$T = \begin{array}{c} \vdots \\ \text{---} \\ \text{---} \\ \text{---} \\ \vdots \end{array} = \boxed{i \text{---} i} . \quad (3.4)$$

It has a global \mathbb{Z}_2 symmetry generated by the operator

$$\eta = \prod_i X_i = \begin{array}{c} \vdots \\ \text{---} \pi \text{---} \\ \text{---} \pi \text{---} \\ \text{---} \pi \text{---} \\ \vdots \end{array} = \boxed{i \text{---} \pi \text{---} i} . \quad (3.5)$$

3.1 Non-invertible Kramers-Wannier duality operator

When $J = h$, known as the critical Ising model, it also has a non-invertible Kramers-Wannier duality symmetry, generated by the operator D which exchanges the Ising and transverse field terms in the Hamiltonian, i.e.,

$$DX_i = Z_i Z_{i+1} D , \quad DZ_i Z_{i+1} = X_{i+1} D . \quad (3.6)$$

There are several equivalent representations of the duality operator. Below we list a few:

1. $D = \frac{1}{\sqrt{2}} e^{-2\pi i L/8} (1 + \eta) e^{\frac{i\pi}{4} X_1} e^{\frac{i\pi}{4} Z_1 Z_2} e^{\frac{i\pi}{4} X_2} e^{\frac{i\pi}{4} Z_2 Z_3} e^{\frac{i\pi}{4} X_3} \dots e^{\frac{i\pi}{4} X_{L-1}} e^{\frac{i\pi}{4} Z_{L-1} Z_L} e^{\frac{i\pi}{4} X_L}$ [81, 14],
2. $D = \frac{1}{2} (1 + \eta) H_1 CZ_{1,2} H_2 CZ_{2,3} H_3 \dots H_{L-1} CZ_{L-1,L} H_L (1 + \eta)$ [15],
3. $D = \text{Tr} (\mathbb{U}^1 \mathbb{U}^2 \dots \mathbb{U}^L)$, where $\mathbb{U}^i = \begin{pmatrix} |0\rangle\langle +|_i & |0\rangle\langle -|_i \\ |1\rangle\langle -|_i & |1\rangle\langle +|_i \end{pmatrix}$ [82, 15], and
4. $D = \sum_{\{m_i\}} | \{ (-)^{m_{i-1}+m_i} \} \rangle \langle \{ m_i \} | = \frac{1}{2^{L/2}} \sum_{\{m_i\}, \{\hat{m}_i\}} (-1)^{\sum_i \hat{m}_i (m_{i-1}+m_i)} | \{ \hat{m}_i \} \rangle \langle \{ m_i \} |$ [13, 83].

between \mathcal{H}_s and \mathcal{H}_1 .

$$\begin{aligned}
D_{1\leftarrow s} &= 2^{L/2} \left[\begin{array}{c} \text{---} i - \frac{1}{2} \\ \circ \\ \text{---} \\ \square \\ \text{---} \\ \circ \\ \text{---} \\ \square \\ \text{---} \\ i \end{array} \right], & T_{1\leftarrow s} &= \left[\begin{array}{c} \text{---} i - \frac{1}{2} \\ \text{---} \\ i \end{array} \right], \\
D_{s\leftarrow 1} &= 2^{L/2} \left[\begin{array}{c} i - \frac{1}{2} \\ \text{---} \\ \circ \\ \text{---} \\ \square \\ \text{---} \\ \circ \\ \text{---} \\ i \end{array} \right], & T_{s\leftarrow 1} &= \left[\begin{array}{c} i - \frac{1}{2} \\ \text{---} \\ i \end{array} \right],
\end{aligned} \tag{3.10}$$

where the sites are labelled by the integer i (modulo L), whereas the links are labelled by the half-integer $i - \frac{1}{2}$ (modulo L). These duality maps were studied in [13, 59, 82, 84, 63, 83]—for instance,

$$D_{1\leftarrow s} \stackrel{\text{SF}}{=} 2^{L/2} \left[\begin{array}{c} \circ \text{---} i - \frac{1}{2} \\ \text{---} \\ \square \\ \text{---} \\ \circ \text{---} \\ \text{---} \\ \square \\ \text{---} \\ i \end{array} \right] = \left(\bigotimes_i \langle + | i \rangle \right) \left(\prod_i \text{CZ}_{i, i - \frac{1}{2}} \text{CZ}_{i, i + \frac{1}{2}} \right) \left(\bigotimes_i | + \rangle_{i + \frac{1}{2}} \right), \tag{3.11}$$

which is the expression for the Kramers-Wannier duality map in terms of the cluster entangler [82, 84]. Furthermore, changing the inputs on sites i to outputs in $D_{1\leftarrow s}$ gives the ZX-diagram of the cluster state associated with the nontrivial $\mathbb{Z}_2 \times \mathbb{Z}_2$ SPT phase.

In terms of these maps, we can write

$$\begin{aligned}
T &= \left[\begin{array}{c} \text{---} \\ \text{---} \\ i \end{array} \right] = T_{s\leftarrow 1} T_{1\leftarrow s}, & D &= 2^{L/2} \left[\begin{array}{c} \text{---} \\ \text{---} \\ \square \\ \text{---} \\ \circ \text{---} \\ \text{---} \\ \square \\ \text{---} \\ i \end{array} \right] = T_{s\leftarrow 1} D_{1\leftarrow s} \\
& & &= 2^{L/2} \left[\begin{array}{c} \text{---} \\ \text{---} \\ \square \\ \text{---} \\ \circ \text{---} \\ \text{---} \\ \square \\ \text{---} \\ i \end{array} \right] = D_{s\leftarrow 1} T_{1\leftarrow s}.
\end{aligned} \tag{3.12}$$

are operators on \mathcal{H}_s .

3.2 Action on operators

Let us compute the action of D on the \mathbb{Z}_2 -symmetric, local operators. Such operators are generated by products of X_i and $Z_i Z_{i+1}$, so it suffices to understand the action on these operators. First, we

have

$$\begin{aligned}
DX_i = 2^{L/2} & \begin{array}{c} \vdots \\ \text{---} \pi \text{---} \\ \vdots \\ i+1 \text{---} \\ \vdots \end{array} \stackrel{\text{Pi}}{\cong} 2^{L/2} \begin{array}{c} \vdots \\ \text{---} \pi \text{---} \\ \text{---} \pi \text{---} \\ \vdots \\ i+1 \text{---} \\ \vdots \end{array} \\
& \stackrel{\text{CC}'}{\cong} 2^{L/2} \begin{array}{c} \vdots \\ \text{---} \pi \text{---} \\ \text{---} \pi \text{---} \\ \vdots \\ i+1 \text{---} \\ \vdots \end{array} \stackrel{\text{SF}}{\cong} 2^{L/2} \begin{array}{c} \vdots \\ \text{---} \pi \text{---} \\ \text{---} \pi \text{---} \\ \vdots \\ i+1 \text{---} \\ \vdots \end{array} = Z_i Z_{i+1} D .
\end{aligned} \tag{3.13}$$

Similarly, one can show that $DZ_i Z_{i+1} = X_{i+1} D$. Therefore, D indeed generates the KW duality transformation.

More generally, for $m_i \in \{0, 1\}$, we have

$$\begin{aligned}
D \prod_i X_i^{m_i} = 2^{L/2} & \begin{array}{c} \vdots \\ \text{---} m_i \pi \text{---} \\ \vdots \\ i+1 \text{---} \\ \vdots \end{array} \stackrel{\text{Pi}}{\cong} 2^{L/2} \begin{array}{c} \vdots \\ \text{---} m_i \pi \text{---} \\ \text{---} m_i \pi \text{---} \\ \vdots \\ i+1 \text{---} \\ \vdots \end{array} \\
& \stackrel{\text{SF}}{\cong} 2^{L/2} \begin{array}{c} \vdots \\ \text{---} (m_i + m_{i-1}) \pi \text{---} \\ \vdots \\ i+1 \text{---} \\ \vdots \end{array} \stackrel{\text{SF, CC}'}{\cong} 2^{L/2} \begin{array}{c} \vdots \\ \text{---} (m_i + m_{i-1}) \pi \text{---} \\ \vdots \\ i+1 \text{---} \\ \vdots \end{array} \\
& = \prod_i Z_i^{m_i + m_{i-1}} D = \prod_i (Z_i Z_{i+1})^{m_i} D ,
\end{aligned} \tag{3.14}$$

and similarly, $D \prod_i (Z_i Z_{i+1})^{m_i} = \prod_i X_{i+1}^{m_i} D$. Consider a special case when $m_1 = m_2 = \dots = m_{k-1} = 1$ for some $k > 2$, and all the other m_i 's are 0. We find that D maps a pair of order

operators (Z) to the disorder operator (X):

$$DZ_1Z_k = X_2X_3 \cdots X_kD . \quad (3.15)$$

Consider an even more special case where $m_i = 1$ for all i , we get

$$D\eta = \eta D = D . \quad (3.16)$$

3.3 Operator algebra

In this subsection, we compute the fusion rules of η , D , and T using ZX-calculus. In particular, we will rederive

$$D^2 = (1 + \eta)T . \quad (3.17)$$

of [14, 15] from ZX-calculus.

The fusion rules involving η and T are:

$$\begin{aligned} \eta^2 &= \boxed{i \text{---} \pi \text{---} \pi \text{---} i} \stackrel{\text{SF}}{=} \boxed{i \text{---} \bullet \text{---} i} \stackrel{\text{I}}{=} \boxed{i \text{---} i} = 1 , \\ T\eta &= \boxed{i \text{---} \pi \text{---} i} = \boxed{i \text{---} \pi \text{---} i} = \eta T , \\ T^L &= \boxed{i \text{---} \dots \text{---} i} = 1 . \end{aligned} \quad (3.18)$$

To see the last line of this equation explicitly, consider $L = 3$ for concreteness:

$$T = \begin{array}{c} 1 \\ 2 \\ 3 \end{array} \left\{ \begin{array}{c} 1 \\ 2 \\ 3 \end{array} \right. \implies T^3 = \begin{array}{c} 1 \\ 2 \\ 3 \end{array} \left\{ \begin{array}{c} 1 \\ 2 \\ 3 \end{array} \right. = \begin{array}{c} 1 \\ 2 \\ 3 \end{array} \left\{ \begin{array}{c} 1 \\ 2 \\ 3 \end{array} \right. = 1 , \quad (3.19)$$

where we colored the wires for clarity.

Let us now compute the fusion rules involving D using ZX-calculus. We already showed that $D\eta = \eta D = D$. Moreover, it is easy to see that D commutes with T . We are then left with the fusion of D with itself:

$$D^2 = D_{s \leftarrow 1} T_{1 \leftarrow s} T_{s \leftarrow 1} D_{1 \leftarrow s} = 2^L \boxed{i \text{---} \begin{array}{c} \bullet \\ \bullet \\ \bullet \end{array} \text{---} i} = 2^L \boxed{i \text{---} \begin{array}{c} \bullet \\ \bullet \\ \bullet \end{array} \text{---} i} = T D_{s \leftarrow 1} D_{1 \leftarrow s} . \quad (3.20)$$

(As an aside, note that $T_{1 \leftarrow s} T_{s \leftarrow 1}$ is the generator of translation on \mathcal{H}_1 .) Similarly, we have

$$D^2 = D_{s \leftarrow 1} D_{1 \leftarrow s} T . \quad (3.21)$$

We now show that $D_{s \leftarrow 1} D_{1 \leftarrow s} = 1 + \eta$ using ZX-calculus:

$$\begin{aligned}
D_{s \leftarrow 1} D_{1 \leftarrow s} &= 2^L \left[\text{Diagram 1} \right] \stackrel{CC'}{\equiv} 2^L \left[\text{Diagram 2} \right] \stackrel{SF}{\equiv} 2^L \left[\text{Diagram 3} \right] \\
&\stackrel{B}{\equiv} \frac{2^L}{2^{L/2}} \left[\text{Diagram 4} \right] \stackrel{SF}{\equiv} 2^{L/2} \left[\text{Diagram 5} \right] =: C,
\end{aligned} \tag{3.22}$$

where C is the condensation operator. It is convenient to define a more general operator

$$C_n := 2^{L/2} \left[\text{Diagram 6} \right], \tag{3.23}$$

where $n = 0$ gives the condensation operator $C = C_0$.

We want to show that $C_n = 1 + (-1)^n \eta$. We have,

$$\begin{aligned}
C_n &= 2^{L/2} \left[\text{Diagram 7} \right] \stackrel{SF}{\equiv} 2^{L/2} \left[\text{Diagram 8} \right] = \frac{2^{L/2}}{2^{L/2}} \cdot (\sqrt{2})^2 \langle (-)^n |_a \left(\prod_{i=1}^L \text{CNOT}_{a,i} \right) | + \rangle_a,
\end{aligned} \tag{3.24}$$

where a represents the auxiliary wire above 1. Now, we have

$$\prod_{i=1}^L \text{CNOT}_{a,i} = \prod_{i=1}^L (|0\rangle\langle 0|_a \otimes I + |1\rangle\langle 1|_a \otimes X_i) = |0\rangle\langle 0|_a \otimes I + |1\rangle\langle 1|_a \otimes \eta. \tag{3.25}$$

It follows that

$$C_n = 2 \langle (-)^n |_a (|0\rangle\langle 0|_a \otimes I + |1\rangle\langle 1|_a \otimes \eta) | + \rangle_a = 1 + (-1)^n \eta. \tag{3.26}$$

Therefore, we proved using ZX-calculus that $C_n = 1 + (-1)^n \eta$, and hence $D^2 = (1 + \eta)T$. More concretely, for $L = 3$, we have

$$\begin{aligned}
D^2 &= 2^{3/2} \left[\text{Diagram 9} \right] = T(1 + \eta) \\
&= 2^{3/2} \left[\text{Diagram 10} \right] = (1 + \eta)T.
\end{aligned} \tag{3.27}$$

It follows from (3.16) that $DC = CD = 2D$. Let us verify this using ZX-calculus:

$$\begin{aligned}
D_{1 \leftarrow s} C = 2^L & \quad \begin{array}{c} \text{Diagram 1} \\ \text{Diagram 2} \end{array} \stackrel{B}{=} 2^L \cdot 2^{L/2} \quad \begin{array}{c} \text{Diagram 3} \\ \text{Diagram 4} \end{array} \\
& \stackrel{SF}{=} 2^{3L/2} \quad \begin{array}{c} \text{Diagram 5} \\ \text{Diagram 6} \end{array} \stackrel{SF}{=} 2^{3L/2} \quad \begin{array}{c} \text{Diagram 7} \\ \text{Diagram 8} \end{array} \\
& \stackrel{SF}{=} 2^{3L/2} \quad \begin{array}{c} \text{Diagram 9} \\ \text{Diagram 10} \end{array} \stackrel{Hf}{=} \frac{2^{3L/2}}{2^L} \quad \begin{array}{c} \text{Diagram 11} \\ \text{Diagram 12} \end{array} \\
& \stackrel{SF}{=} 2^{L/2} \quad \begin{array}{c} \text{Diagram 13} \\ \text{Diagram 14} \end{array} \stackrel{S}{=} 2 \cdot 2^{L/2} \quad \begin{array}{c} \text{Diagram 15} \\ \text{Diagram 16} \end{array} = 2D_{1 \leftarrow s} .
\end{aligned} \tag{3.28}$$

Multiplying $T_{s \leftarrow 1}$ on the left on both sides gives the desired fusion rule. Showing that $CD = 2D$ is similar.

For the sake of completeness, let us also compute $C^2 = 2C$ using ZX-calculus:

$$\begin{aligned}
C^2 = 2^L & \quad \begin{array}{c} \text{Diagram 1} \\ \text{Diagram 2} \end{array} \stackrel{SF}{=} 2^L \quad \begin{array}{c} \text{Diagram 3} \\ \text{Diagram 4} \end{array} \stackrel{GB}{=} \frac{2^L}{2^{(L-1)/2}} \quad \begin{array}{c} \text{Diagram 5} \\ \text{Diagram 6} \end{array} \\
& \stackrel{SC, SF}{=} \frac{2^{(L+1)/2}}{\sqrt{2}} \quad \begin{array}{c} \text{Diagram 7} \\ \text{Diagram 8} \end{array} \stackrel{S}{=} 2 \cdot 2^{L/2} \quad \begin{array}{c} \text{Diagram 9} \\ \text{Diagram 10} \end{array} = 2C .
\end{aligned} \tag{3.29}$$

3.4 Action on states

The phase diagram of the Ising model (3.3) is well-understood [85]: the \mathbb{Z}_2 global symmetry is spontaneously broken (ferromagnetic phase) for $J > h$, whereas it is preserved (paramagnetic phase) for $J < h$. At the critical point $J = h$, there is a second order phase transition captured by the Ising CFT at low energies.

Let us comment on the ground states and the superselection sectors in these phases. In the limit $J \gg h$ (or when $h = 0$), the Ising term dominates. In finite volume, there are two low-lying states whose energy splitting is exponentially small in L . In infinite volume, the Hilbert space splits into two superselection sectors:

$$|0 \cdots 0\rangle , \quad |1 \cdots 1\rangle , \tag{3.30}$$

On the other hand, in the limit $J \ll h$ (or when $J = 0$), the transverse field term dominates, so

there is a unique ground state,

$$|+\cdots+\rangle. \quad (3.31)$$

In fact, these three product states $|0\cdots 0\rangle, |1\cdots 1\rangle, |+\cdots+\rangle$ are the exact ground states of a special case ($\lambda = 1$) of the lattice model introduced in [80]:

$$H_\lambda = -J \left[\sum_i (Z_i Z_{i+1} + X_i) - \frac{\lambda}{2} \sum_i (X_{i-1} Z_i Z_{i+1} + Z_i Z_{i+1} X_{i+2}) \right]. \quad (3.32)$$

For any λ , this Hamiltonian preserves both the \mathbb{Z}_2 and the KW duality symmetries. In the thermodynamic limit, the model is in the $c = 1/2$ Ising CFT phase for $0 \leq \lambda \lesssim 0.856$, reaches the $c = 7/10$ tricritical Ising CFT point at $\lambda \sim 0.856$, and becomes gapped with three superselection sectors for $\lambda \gtrsim 0.856$. These phases are consistent with the LSM-type constraint from the non-invertible symmetry in [15]. In particular, this model was shown to have exact three-fold degeneracy even at finite L when $\lambda = 1$.

Irrespective of the Hamiltonian, one can ask how the symmetry operators η and D act on these states [15]:

$$\begin{aligned} \eta|0\cdots 0\rangle &= |1\cdots 1\rangle, & \eta|1\cdots 1\rangle &= |0\cdots 0\rangle, & \eta|+\cdots+\rangle &= |+\cdots+\rangle, \\ D|0\cdots 0\rangle &= D|1\cdots 1\rangle = |+\cdots+\rangle, & D|+\cdots+\rangle &= |0\cdots 0\rangle + |1\cdots 1\rangle. \end{aligned} \quad (3.33)$$

This basis corresponds to the three superselection sectors of the Hamiltonian (3.32) in the thermodynamic limit. Alternatively, one can work in a basis that diagonalizes the symmetry operators:

$$\begin{aligned} \frac{1}{\sqrt{2}}|+\cdots+\rangle \pm \frac{1}{\sqrt{2}}|\text{GHZ}^+\rangle, & \quad D = \pm\sqrt{2}, \eta = 1, \\ |\text{GHZ}^-\rangle, & \quad D = 0, \eta = -1, \end{aligned} \quad (3.34)$$

where

$$|\text{GHZ}^\pm\rangle := \frac{1}{\sqrt{2}}(|0\cdots 0\rangle \pm |1\cdots 1\rangle). \quad (3.35)$$

The duality operator exchanges $|\text{GHZ}^+\rangle$ with the product state $|+\cdots+\rangle$:

$$D|+\cdots+\rangle = \sqrt{2}|\text{GHZ}^+\rangle, \quad D|\text{GHZ}^+\rangle = \sqrt{2}|+\cdots+\rangle. \quad (3.36)$$

4 Review of 3+1d lattice \mathbb{Z}_2 gauge theory

We denote the sites, links, plaquettes, and cubes of a 3d cubic lattice by s, ℓ, p, c , respectively. Let L_x, L_y, L_z be the number of sites in each direction and assume periodic boundary conditions. We place a qubit associated with a local Hilbert space $\mathcal{H}_\ell \cong \mathbb{C}^2$ on every link. It is the \mathbb{Z}_2 1-form gauge field. We denote the Pauli operators acting on link ℓ as X_ℓ, Z_ℓ . The total Hilbert space is $\mathcal{H} = \bigotimes_\ell \mathcal{H}_\ell$.

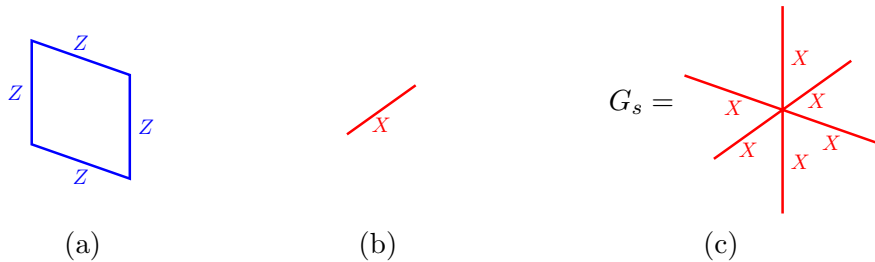


Figure 2: The local terms and the Gauss law of the Hamiltonian (4.2) of the lattice \mathbb{Z}_2 gauge theory. (a) The magnetic flux term on a plaquette (first term of (4.2)), (b) the electric field term on a link (second term of (4.2)), and (c) the Gauss law operator G_s at a site.

Next, we impose the Gauss law for the \mathbb{Z}_2 1-form gauge field strictly as an operator equation at every site:

$$G_s = \prod_{\ell \ni s} X_\ell = 1 . \quad (4.1)$$

We denote the Hilbert space subject to this constraint as $\tilde{\mathcal{H}}$, which is not a tensor product of local factors. We will later relax this operator equation and impose it energetically.

We start with the standard Hamiltonian for the lattice gauge theory:

$$\tilde{H} = -J \sum_p \prod_{\ell \in p} Z_\ell - h \sum_\ell X_\ell , \quad (4.2)$$

which acts on the constrained Hilbert space $\tilde{\mathcal{H}}$. The first term is the analog of the magnetic flux term, while the second term is the analog of the electric field term in the continuum. (See Figure 2 for an illustration of these terms.) We will later study deformations of this Hamiltonian while preserving all the symmetries of interest.

4.1 Topological versus non-topological 1-form global symmetries

The central global symmetry that will be important to us is a lattice global symmetry generated by

$$\eta(\hat{\Sigma}) = \prod_{\ell \in \hat{\Sigma}} X_\ell , \quad (4.3)$$

where $\hat{\Sigma}$ is a 2-dimensional surface on the dual lattice. The product is over all the links orthogonal to $\hat{\Sigma}$, or equivalently, over all the dual plaquettes on $\hat{\Sigma}$. In contrast to an ordinary global symmetry, this symmetry operator acts only on part of the space and commutes with the Hamiltonian \tilde{H} for any $\hat{\Sigma}$. Since the symmetry operator is a product of the electric field X_ℓ on a codimension-1 surface in the 3-dimensional space, we refer to it as an electric 1-form global symmetry denoted by $\mathbb{Z}_2^{(1)}$. (The superscript stands for the codimension of the symmetry operator in space.)

When the Gauss law is imposed as a strict operator equation as in (4.1), this 1-form global

symmetry is *topological* in the sense that

$$\eta(\widehat{\Sigma}) = \eta(\widehat{\Sigma}') , \quad \text{if } \widehat{\Sigma} \sim \widehat{\Sigma}' , \quad (4.4)$$

where $\widehat{\Sigma} \sim \widehat{\Sigma}'$ means that they are in the same homology class on the dual lattice. That is, the symmetry operator depends only on the homological class of the 2-cycle $\widehat{\Sigma}$. Therefore, the \mathbb{Z}_2 1-form symmetry is generated by the operators associated with the three fundamental non-contractible surfaces.

Similar to the continuum, this topological 1-form symmetry cannot be violated by any local operator deformation to the Hamiltonian. For instance, a term like Z_ℓ violates the Gauss law (4.1) and is excluded from the Hamiltonian as a valid deformation.

Alternatively, we can relax the Gauss law constraint (4.1), and impose it energetically in the Hamiltonian as:

$$H = -J \sum_p \prod_{\ell \in p} Z_\ell - h \sum_\ell X_\ell - g \sum_s \prod_{\ell \ni s} X_\ell . \quad (4.5)$$

This Hamiltonian acts on the tensor product Hilbert space \mathcal{H} . When $g \rightarrow \infty$, it reduces to the previous case where the Gauss law is enforced strictly. When $h = 0$, this is the 3+1d toric code.⁸

When the Gauss law is relaxed such as in H , the 1-form symmetry is no longer topological: $\eta(\widehat{\Sigma})$ is a distinct operator acting on \mathcal{H} for each dual surface $\widehat{\Sigma}$. Now that the Gauss law is relaxed, the non-topological 1-form symmetry can be violated by local operators, such as Z_ℓ . The difference between topological and non-topological higher-form symmetries on the lattice have been previously discussed in [87, 88, 44].⁹

This is a general feature: a higher-form global symmetry in the continuum, or a topological higher-form symmetry on the lattice cannot be violated by local operators. On the other hand, a non-topological one on the lattice can be violated by local operator deformations.

4.2 Defects for the 1-form symmetry

Having discussed the conserved operator $\eta(\widehat{\Sigma})$, we move on to the defect for the 1-form symmetry on the lattice. We work with the more general system where the Gauss law is only enforced energetically. The 1-form symmetry defect is represented as a modification of the Hamiltonian along a curve $\widehat{\gamma}$ on the dual lattice. We refer to the Hamiltonian with a defect as the defect

⁸Moreover, the model with $h = 0$ has an additional (non-topological) magnetic 2-form symmetry. This is analogous to the (topological) 1-form and 2-form symmetries in the modified Villain (integer BF) Euclidean lattice model for the 3+1d \mathbb{Z}_2 gauge theory [86].

⁹Topological/non-topological 1-form symmetries are respectively referred to as relativistic/non-relativistic 1-form symmetries in [87], and as non-faithful/faithful in [88]. Here we adopt the terminology topological/non-topological symmetries as in [44] because it directly reflects the property of the operators.

Hamiltonian, which is given by

$$H_\eta(\widehat{\gamma}) = -J \sum_p (-1)^{\langle \widehat{\gamma}, p \rangle} \prod_{\ell \in p} Z_\ell - h \sum_\ell X_\ell - g \sum_s \prod_{\ell \ni s} X_\ell, \quad (4.6)$$

where $\langle \widehat{\gamma}, p \rangle$ is the intersection number of $\widehat{\gamma}$ and p . The subscript and the superscript stand for the type and the location of the defect, respectively. The defect is topological in the sense that we can move its location by a product of local unitaries. Specifically, let $\widehat{\gamma}'$ be another curve that is homological to $\widehat{\gamma}$, and let $\widehat{\Sigma}$ be the surface bounded by $\widehat{\gamma} - \widehat{\gamma}'$. Then

$$\left(\prod_{\ell \in \widehat{\Sigma}} X_\ell \right) H_\eta(\widehat{\gamma}) \left(\prod_{\ell \in \widehat{\Sigma}} X_\ell \right)^{-1} = H_\eta(\widehat{\gamma}'). \quad (4.7)$$

where the product is over all dual faces, or equivalently, links ℓ , lying on the dual surface $\widehat{\Sigma}$. Note that even though the 1-form symmetry operator $\eta(\widehat{\Sigma})$ is not topological, the associated defect is.

4.3 Gauging the 1-form symmetry and the Wegner duality

The 1-form symmetry (4.3) is on-site [89] and is free of 't Hooft anomaly. It means that it is compatible with a trivially gapped phase, and it can be gauged. Here, we gauge the 1-form global symmetry, following the discussion in Appendix B of [51] and Sec. IIIB of [90]. This generalizes the prescription for gauging a 0-form symmetry outlined in [91, 15].

For concreteness, we focus on the Hamiltonian in (4.2), but most of the conclusions hold true for more general Hamiltonian invariant under the 1-form symmetry. The local term of such a general Hamiltonian is a product of X_ℓ and $\prod_{\ell \in p} Z_\ell$.

We gauge the 1-form global symmetry η by introducing a qubit with Pauli operators σ_p^a ($a = x, y, z$) on every plaquette p . In the continuum, they represent the 2-form \mathbb{Z}_2 gauge fields for the 1-form symmetry. The gauging consists of three steps:

1. Gauss law: Impose the Gauss law for the 2-form gauge field at every link:

$$G_\ell = X_\ell \prod_{p \ni \ell} \sigma_p^z = 1. \quad (4.8)$$

With this new Gauss law, the original one $G_s = \prod_{\ell \ni s} X_\ell = 1$ is trivially satisfied, and we no longer have to impose the latter by hand.

2. Minimal coupling: Couple the gauge fields minimally to the Hamiltonian by replacing the plaquette term $\prod_{\ell \in p} Z_\ell$ by $\sigma_p^x \prod_{\ell \in p} Z_\ell$.
3. Flux term: We add a gauge-invariant term $\prod_{p \in c} \sigma_p^x$ of the 2-form gauge fields for every cube to the Hamiltonian. This term is analogous to the magnetic field square term in the continuum.

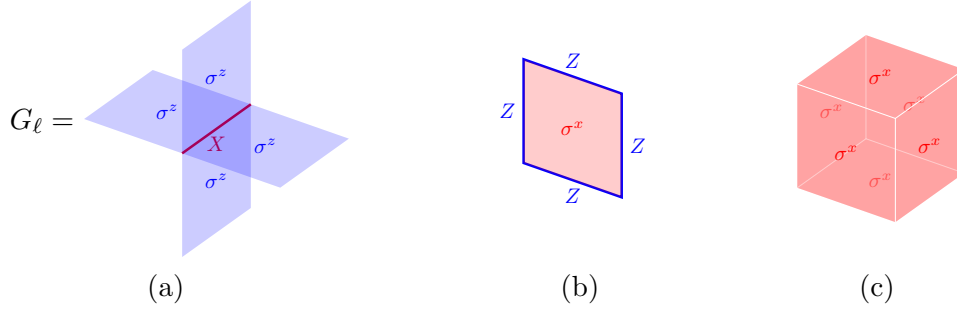


Figure 3: The Gauss law and the local terms of the gauged Hamiltonian (4.9). (a) The Gauss law operator G_ℓ for the 2-form gauge field on a link, (b) the minimal coupling term on a plaquette (first term of (4.9)), and (c) the flux term of the 2-form gauge field on a cube (third term of (4.9)). The second term of (4.9) is the same as Figure 2(b).

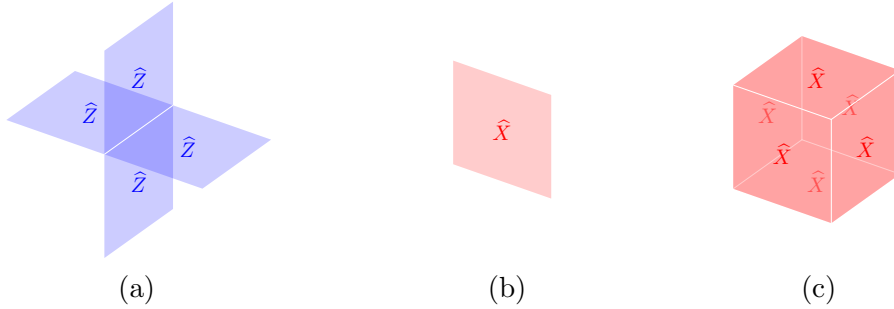


Figure 4: The local terms and the Gauss law of the gauged Hamiltonian (4.9) in the new variables. (a) The dual magnetic flux term on a link (second term of (4.12)), (b) the dual electric field term on a plaquette (first term of (4.12)), and (c) the dual Gauss law operator on a cube (third term of (4.12)).

The gauged Hamiltonian is then

$$\hat{H} = -J \sum_p \sigma_p^x \prod_{\ell \in p} Z_\ell - h \sum_\ell X_\ell - \hat{g} \sum_c \prod_{p \in c} \sigma_p^x, \quad (4.9)$$

subject to the Gauss law constraint for the 2-form gauge fields:

$$G_\ell = X_\ell \prod_{p \ni \ell} \sigma_p^z = 1. \quad (4.10)$$

See Figure 3 for an illustration of these terms.

Next, we define a new set of gauge-invariant local operators that commute with the Gauss law G_ℓ :

$$\hat{X}_p = \sigma_p^x \prod_{\ell \in p} Z_\ell, \quad \hat{Z}_p = \sigma_p^z. \quad (4.11)$$

The gauged Hamiltonian written in terms of the new variables is

$$\widehat{H} = -J \sum_p \widehat{X}_p - h \sum_\ell \prod_{p \ni \ell} \widehat{Z}_p - \widehat{g} \sum_c \prod_{p \in c} \widehat{X}_p . \quad (4.12)$$

(See Figure 4 for an illustration of these terms.) If we dualize the lattice, this becomes the Hamiltonian of a lattice \mathbb{Z}_2 gauge field theory. The last term is interpreted as the Gauss law for the hatted gauge fields imposed dynamically. The gauged Hamiltonian has a dual, non-topological 1-form symmetry, generated by

$$\widehat{\eta}(\Sigma) = \prod_{p \in \Sigma} \widehat{X}_p , \quad (4.13)$$

where Σ is a closed 2-cycle of the original lattice. Note that this dual symmetry exists whether we impose the Gauss law (4.1) for the 1-form gauge field exactly or energetically.

Finally, we consider the limit $\widehat{g} \rightarrow \infty$, which sets the 2-form gauge fields to be topological. Furthermore, the dual 1-form symmetry $\widehat{\eta}$ becomes topological, i.e., it depends on Σ only through its homological class. We refer to the gauging procedure with $\widehat{g} \rightarrow \infty$ as the *topological gauging* of the 1-form symmetry.

In this limit, we retrieve the original Hamiltonian on the dual lattice before gauging with $J \leftrightarrow h$. We conclude that the \mathbb{Z}_2 lattice gauge theory is self-dual under the topological gauging when $J = h$. This is the Wegner duality for the 3+1d \mathbb{Z}_2 lattice gauge theory [47], generalizing the Kramers-Wannier duality for the 1+1d Ising lattice model.

To summarize, we see that the topological gauging of the 1-form symmetry maps the local terms in the Hamiltonian as

$$X_\ell \rightsquigarrow \prod_{p \ni \ell} \widehat{Z}_p , \quad \prod_{\ell \in p} Z_\ell \rightsquigarrow \widehat{X}_p , \quad (4.14)$$

which is the Wegner duality transformation.

5 Non-invertible Wegner operator in 3+1d

When $J = h$, the Hamiltonian (4.2) for the lattice \mathbb{Z}_2 gauge theory:

$$\widetilde{H} = -J \left(\sum_p \prod_{\ell \in p} Z_\ell + \sum_\ell X_\ell \right) , \quad (5.1)$$

is invariant under the Wegner duality transformation (4.14),

$$X_\ell \rightsquigarrow \prod_{\ell' \in \mathfrak{t}(\ell)} Z_{\ell'} , \quad \prod_{\ell \in p} Z_\ell \rightsquigarrow X_{\mathfrak{t}(p)} , \quad (5.2)$$

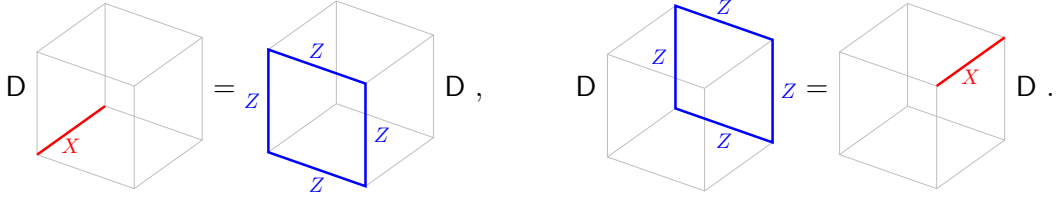


Figure 5: Action of the duality operator D on the terms of the Hamiltonian \tilde{H} .

up to a half lattice translation \mathfrak{t} :

$$\mathfrak{t}(x, y, z) = (x + \frac{1}{2}, y + \frac{1}{2}, z + \frac{1}{2}) , \quad (5.3)$$

where $(x, y, z) \in (\mathbb{Z}/L_x\mathbb{Z}, \mathbb{Z}/L_y\mathbb{Z}, \mathbb{Z}/L_z\mathbb{Z})$ labels a site on the lattice, and so on.

However, this transformation (5.2) cannot be implemented by an invertible operator on a closed periodic torus. Suppose there were such an invertible operator U such that $UX_\ell U^{-1} = \prod_{\ell' \in \mathfrak{t}(\ell)} Z_{\ell'}$. Then consider the conjugation of the 1-form symmetry operator $\eta(\widehat{\Sigma})$ by U :

$$U\eta(\widehat{\Sigma})U^{-1} = U \left(\prod_{\ell \in \widehat{\Sigma}} X_\ell \right) U^{-1} = \prod_{\ell \in \widehat{\Sigma}} \prod_{\ell' \in \mathfrak{t}(\ell)} Z_{\ell'} = 1 . \quad (5.4)$$

This implies the 1-form symmetry operator η is trivial, which is a contradiction.

Rather, the transformation (5.2) is implemented by a non-invertible operator D in the following sense

$$DX_\ell = \left(\prod_{\ell' \in \mathfrak{t}(\ell)} Z_{\ell'} \right) D , \quad D \prod_{\ell \in p} Z_\ell = X_{\mathfrak{t}(p)} D . \quad (5.5)$$

See Figure 5 for an illustration of the action of D on the terms of the Hamiltonian (4.2). It follows from (5.5) that

$$D\eta(\widehat{\Sigma}) = \eta(\widehat{\Sigma})D = D , \quad (5.6)$$

which in particular implies $DG_s = G_s D = D$. This means that the operator D acts within the constrained Hilbert space $\tilde{\mathcal{H}}$, i.e., the subspace of \mathcal{H} with $G_s = 1$.

From these relations, for $J = h$, we see that this operator D commutes with the Hamiltonian H in (4.5):

$$H = -J \left(\sum_p \prod_{\ell \in p} Z_\ell + \sum_\ell X_\ell \right) - g \sum_s \prod_{\ell \ni s} X_\ell \quad (5.7)$$

even when the Gauss law is only imposed energetically. That is, $DH = HD$. We will henceforth view D as an operator acting on the tensor product Hilbert space $\mathcal{H} = \bigotimes_\ell \mathcal{H}_\ell$.

Moreover, we have

$$D^2 X_\ell = X_{t^2(\ell)} D^2, \quad D^2 \prod_{\ell \in p} Z_\ell = \left(\prod_{\ell \in t^2(p)} Z_\ell \right) D^2. \quad (5.8)$$

The algebra (5.6) and (5.8) suggests that D^2 is proportional to a projection onto the Gauss-law-preserving, $\mathbb{Z}_2^{(1)}$ -symmetric states times $T_{1,1,1}$, which is the generator of translation in the $(1, 1, 1)$ direction.

In the following subsections, we will make the last statement more precise. Specifically, we give an explicit realization of the duality operator D in terms of ZX-diagrams, and compute its fusion algebra with itself and other operators using ZX-calculus.

5.1 Non-invertible duality symmetry as a tensor network operator

In this subsection, we give a ZX-diagrammatic representation of the duality operator D . Our operator D in the 3+1d Hamiltonian lattice gauge theory is the counterpart of the duality defect for the 4d Euclidean lattice gauge theory of [50].

First, we define an auxiliary Hilbert space on the plaquettes \mathcal{H}_p in the same way as the Hilbert space on the links defined above, which we now denote as \mathcal{H}_l for clarity. Consider the following maps between \mathcal{H}_l and \mathcal{H}_p :

$$D_{p \leftarrow l} := 2^{4V} \text{ (left diagram)}, \quad D_{l \leftarrow p} := 2^{4V} \text{ (right diagram)}, \quad (5.9)$$

where $V = L_x L_y L_z$ is the number of unit cells in the lattice, the ingoing (outgoing) arrows represent inputs (outputs), the thick gray lines represent the links of the cubic lattice (in particular, the green dots are not the sites of the lattice), and the diagram is repeated and glued in a periodic way in the three spatial directions. These maps have been considered in [92].

We also define the *half-translation* map $T_{p \leftarrow l}$ which maps a qubit in \mathcal{H}_l on the link ℓ to a qubit in \mathcal{H}_p on the plaquette $t(\ell)$. The other half-translation map $T_{l \leftarrow p}$ is defined similarly.

With these preparations, the duality operator is defined as

$$D := T_{l \leftarrow p} D_{p \leftarrow l} = D_{l \leftarrow p} T_{p \leftarrow l}. \quad (5.10)$$

We can also write the translation generator in the $(1, 1, 1)$ direction as

$$T_{1,1,1} = T_{1 \leftarrow p} T_{p \leftarrow 1} . \quad (5.11)$$

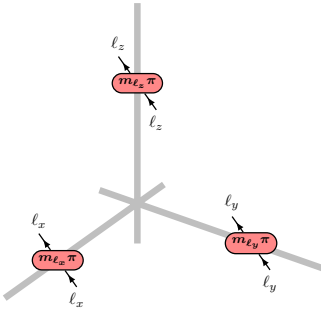
Similarly, there are auxiliary versions of these operators that act on \mathcal{H}_p :

$$\widehat{T}_{1,1,1} = T_{p \leftarrow 1} T_{1 \leftarrow p} , \quad \widehat{D} := T_{p \leftarrow 1} D_{1 \leftarrow p} = D_{p \leftarrow 1} T_{1 \leftarrow p} . \quad (5.12)$$

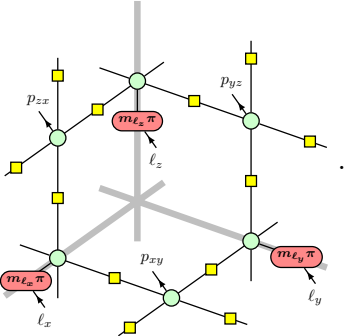
Equation (5.10) expresses the Wegner duality operator as a *tensor network operator*, also known as the *projected entangled pair operator* (PEPO) [54]. This is a higher dimensional generalization of the MPO presentation of the 1+1d Kramers-Wannier operator.¹⁰

5.2 Action on operators

Let us show that D defined in (5.10) is indeed the duality operator, i.e., it satisfies (5.5), using ZX-calculus. It turns out to be more convenient to consider the action of D on a more general operator

$$\prod_{\ell} X_{\ell}^{m_{\ell}} = \quad , \quad m_{\ell} \in \{0, 1\} . \quad (5.13)$$


We have

$$D_{p \leftarrow 1} \prod_{\ell} X_{\ell}^{m_{\ell}} = 2^{4V} \quad (5.14)$$


¹⁰The relation between D and quantum cellular automata will be discussed in [93].

Using π commutation Pi through the green dots on the links or identity removal I, followed by color change CC', and finally spider fusion SF through the green dots on the plaquettes, we get

$$\mathbb{D}_{p \leftarrow 1} \prod_{\ell} X_{\ell}^{m_{\ell}} = 2^{4V} = \prod_p \widehat{Z}_p^{(dm)_p} \mathbb{D}_{p \leftarrow 1}, \quad (5.15)$$

where $(dm)_p := \sum_{\ell \in p} m_{\ell}$ is the sum of m_{ℓ} over the links ℓ around the plaquette p and \widehat{Z}_p is a Pauli operator on the auxiliary Hilbert space \mathcal{H}_p . Multiplying $T_{1 \leftarrow p}$ on the left on both sides of this equation, we get

$$\mathbb{D} \prod_{\ell} X_{\ell}^{m_{\ell}} = T_{1 \leftarrow p} \prod_p \widehat{Z}_p^{(dm)_p} \mathbb{D}_{p \leftarrow 1} = \prod_{\ell'} Z_{\ell'}^{(dm)_{\mathfrak{t}^{-1}(\ell')}} \mathbb{D} = \prod_{\ell} \left(\prod_{\ell' \in \mathfrak{t}(\ell)} Z_{\ell'} \right)^{m_{\ell}} \mathbb{D}, \quad (5.16)$$

where, in the second equality, we used $T_{1 \leftarrow p} \widehat{Z}_p = Z_{\mathfrak{t}(p)} T_{1 \leftarrow p}$, and in the last equality, we used $\ell \in \mathfrak{t}^{-1}(\ell') \iff \ell' \in \mathfrak{t}(\ell)$.¹¹ This in particular implies the first equation of (5.5). Similarly, one can show that $\mathbb{D} \prod_{\ell \in p} Z_{\ell} = X_{\mathfrak{t}(p)} \mathbb{D}$, or more generally,

$$\mathbb{D} \prod_p \left(\prod_{\ell \in p} Z_{\ell} \right)^{\hat{m}_p} = \prod_p X_{\mathfrak{t}(p)}^{\hat{m}_p} \mathbb{D}. \quad (5.17)$$

Therefore, \mathbb{D} is indeed the duality operator which satisfies (5.5).

Let us look at some special cases of the action of \mathbb{D} .

- Let γ be a closed contractible curve bounding the open surface Σ . In the special case where $\hat{m}_p = 1$ for $p \in \Sigma$ and 0 otherwise, (5.17) reduces to

$$\mathbb{D} \prod_{\ell \in \gamma} Z_{\ell} = \prod_{\ell \in \mathfrak{t}(\Sigma)} X_{\ell} \mathbb{D}, \quad (5.18)$$

where $\mathfrak{t}(\Sigma)$ is an open dual surface with boundary $\mathfrak{t}(\gamma)$. This is illustrated in Figure 6. We

¹¹Recall that $\mathfrak{t}(p)$ is the link obtained from the plaquette p by $(\frac{1}{2}, \frac{1}{2}, \frac{1}{2})$, and $\mathfrak{t}(\ell)$ is the plaquette obtained by translating from the link ℓ by $(\frac{1}{2}, \frac{1}{2}, \frac{1}{2})$.

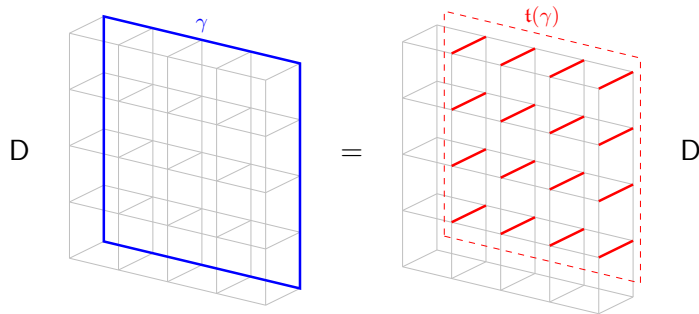


Figure 6: The duality operator D maps a (contractible) Wilson loop along γ to a truncated \mathbb{Z}_2 1-form symmetry operator on the open dual surface $\mathfrak{t}(\Sigma)$ with boundary $\mathfrak{t}(\gamma)$. Here, the blue (red) links correspond to the Pauli Z (X) operators.

recognize the operator on the left hand side as the Wilson line operator along the curve γ ¹²

$$W(\gamma) := \prod_{\ell \in \gamma} Z_\ell , \quad (5.19)$$

whereas the operator on the right hand side is a truncated \mathbb{Z}_2 1-form symmetry operator along the open dual surface $\mathfrak{t}(\Sigma)$ with boundary $\mathfrak{t}(\gamma)$. This equation is, therefore, the lattice counterpart of the continuum result in [51, 94]. In particular, see Figure 1 of [94].

- In the special case where m_ℓ is such that $(dm)_p = 0 \pmod{2}$ for all p , i.e., if m_ℓ is a flat \mathbb{Z}_2 gauge field configuration, then (5.16) reduces to $D \prod_\ell X_\ell^{m_\ell} = D$. This is indeed the case for G_s and $\eta(\widehat{\Sigma})$, so we have $DG_s = D\eta(\widehat{\Sigma}) = D$. Similarly, one can show that $G_s D = \eta(\widehat{\Sigma})D = D$. These reproduce the algebra in (5.6) using ZX-calculus.

5.3 Operator algebra and the condensation operator

Here we summarize the operator algebra of the Wegner duality operator D and the 1-form symmetry operator η . The most interesting one is

$$D^2 = \frac{1}{2^V} T_{1,1,1} \sum_{\widehat{\Sigma}} \eta(\widehat{\Sigma}) , \quad (5.20)$$

where the sum is over all (contractible and non-contractible, and not necessarily connected) 2-cycles $\widehat{\Sigma}$ on the dual lattice. It is the 3+1d generalization of $D^2 = (1 + \eta)T$ (3.17) found in [14, 15]. We derive this algebra in Appendix A.2 using ZX-calculus.

¹²The Wilson line operator, which is charged under the \mathbb{Z}_2 1-form symmetry, is well-defined even when γ is non-contractible.

The other equations are¹³

$$\begin{aligned} D^\dagger &= D T_{1,1,1}^{-1} = T_{1,1,1}^{-1} D , \\ \eta(\widehat{\Sigma})^2 &= 1 , \quad \eta(\widehat{\Sigma}) D = D \eta(\widehat{\Sigma}) = D . \end{aligned} \quad (5.22)$$

It is useful to define the condensation operator:

$$C = \frac{1}{2^V} \sum_{\widehat{\Sigma}} \eta(\widehat{\Sigma}) . \quad (5.23)$$

We can decompose the sum over all 2-cycles into a sum over the non-contractible 2-cycles times a sum over all contractible surfaces:

$$\frac{1}{2^V} \sum_{\widehat{\Sigma}} \eta(\widehat{\Sigma}) = \frac{1}{2} \prod_{i < j} (1 + \eta_{ij}) \prod_{s \neq s_0} \left(\frac{1 + G_s}{2} \right) , \quad (5.24)$$

where s_0 is an arbitrary site and $G_s = \prod_{\ell \ni s} X_\ell$. Here, η_{ij} is the 1-form symmetry operator on the ij -plane, defined as

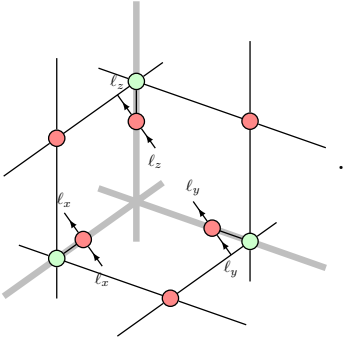
$$\eta_{ij} = \eta(\widehat{\Sigma}_{ij}) = \prod_{\ell \in \widehat{\Sigma}_{ij}} X_\ell , \quad (5.25)$$

Using $\prod_s G_s = 1$, we can include the factor $\frac{1+G_{s_0}}{2}$ for free to obtain

$$C = \frac{1}{2} (1 + \eta_{xy})(1 + \eta_{yz})(1 + \eta_{zx}) \prod_s \left(\frac{1 + G_s}{2} \right) . \quad (5.26)$$

In Appendix A.1, we further show that C can be diagrammatically represented as

$C = 2^{7V/2}$



$. \quad (5.27)$

¹³The first line is obtained as follows: first, the ZX-diagram of $(D_{p \leftarrow 1})^\dagger$ is obtained by reversing the arrows (exchanging inputs/outputs) in the diagram of $D_{p \leftarrow 1}$ (since there are no nontrivial phases in any of the spiders, flipping the signs of the phases does not change the diagram). It is clear that the resulting diagram is the same as that of $D_{1 \leftarrow p}$, so $(D_{p \leftarrow 1})^\dagger = D_{1 \leftarrow p}$. It follows that

$$D^\dagger = (D_{p \leftarrow 1})^\dagger (T_{1 \leftarrow p})^\dagger = D_{1 \leftarrow p} (T_{1 \leftarrow p})^\dagger = D_{1 \leftarrow p} T_{p \leftarrow 1} (T_{p \leftarrow 1})^\dagger (T_{1 \leftarrow p})^\dagger = D T_{1,1,1}^{-1} . \quad (5.21)$$

Similarly, it can be shown that $D^\dagger = T_{1,1,1}^{-1} D$.

In terms of the condensation operator, (5.20) can be rewritten as

$$D^2 = C T_{1,1,1} . \quad (5.28)$$

Using (5.6) and (5.26), we also find

$$C^2 = 4C , \quad DC = CD = 4D . \quad (5.29)$$

Furthermore,

$$C \eta(\widehat{\Sigma}) = \eta(\widehat{\Sigma}) C = C , \quad (5.30)$$

follows immediately from writing $C = D^2 T_{1,1,1}^{-1}$ and (5.6). (Here, we have used the fact that $T_{1,1,1}$ commutes with all the operators.) This in particular implies $CG_s = G_s C = C$.

Let us now compare the lattice algebra with the continuum one. In the thermodynamic limit, $T_{1,1,1} \sim 1$ becomes the identity operator on the low-lying states, and (5.20) reduces to the algebra of the duality operator $\mathcal{D}(M)$ in continuum field theory [51, 52, 95]:¹⁴

$$\mathcal{D}(M)^2 = \frac{1}{|H^0(M; \mathbb{Z}_2)|} \sum_{\Sigma \in H_2(M; \mathbb{Z}_2)} \eta(\Sigma) . \quad (5.31)$$

Here, M is the spatial 3-manifold, which in our case is T^3 .

Next, we compare the condensation operators in the continuum and on the lattice. When restricted to the constrained Hilbert space $\widetilde{\mathcal{H}}$ where the Gauss law is strictly enforced $G_s = 1$, the lattice condensation operator (5.26) reduces to $\frac{1}{2}(1 + \eta_{xy})(1 + \eta_{yz})(1 + \eta_{zx})$. This agrees with the definition of the condensation operator $\mathcal{C}(M)$ in continuum field theory [95] (see also [96])

$$\mathcal{C}(M) = \frac{1}{|H^0(M; \mathbb{Z}_2)|} \sum_{\Sigma \in H_2(M; \mathbb{Z}_2)} \eta(\Sigma) . \quad (5.32)$$

Finally, the full algebra of the condensation and duality operators in the continuum is [95]

$$\begin{aligned} \mathcal{D}(M)^2 &= \mathcal{C}(M) , & \mathcal{C}(M)^2 &= (\mathcal{Z}_2)_0 \mathcal{C}(M) , \\ \mathcal{D}(M) \times \mathcal{C}(M) &= \mathcal{C}(M) \times \mathcal{D}(M) = (\mathcal{Z}_2)_0 \mathcal{D}(M) , \end{aligned} \quad (5.33)$$

where $(\mathcal{Z}_2)_0$ stands for the partition function of the untwisted 2+1d \mathbb{Z}_2 gauge theory (i.e., the low energy limit of the 2+1d toric code) on M . In our case, $M = T^3$, and $(\mathcal{Z}_2)_0=4$, reflecting the four anyon lines. This algebra agrees with the lattice operator algebra in (5.28) and (5.29) in the thermodynamic limit, where the lattice translation $T_{1,1,1} \sim 1$ becomes the identity operator on the low-lying states. See [7] for a review of the duality and condensation operators/defects in

¹⁴The continuum duality operator is self-adjoint, $\mathcal{D}(M) = \mathcal{D}(M)^\dagger$, but on the lattice D^\dagger and D differ by a lattice translation $T_{1,1,1}$. In the continuum, the duality operator associated with a $\mathbb{Z}_N^{(1)}$ symmetry with $N > 2$ is not self-adjoint; \mathcal{D} and \mathcal{D}^\dagger differ by a charge conjugation.

continuum field theory.

5.4 Lattice symmetries

The presence of the lattice translation $T_{1,1,1}$ in (5.20) leads to an interesting action of lattice symmetries on the duality operator D . The ZX-diagram of D makes the translation invariance manifest, i.e.,

$$DT_{\mathbf{a}} = T_{\mathbf{a}}D, \quad \mathbf{a} \in \mathbb{Z}^3. \quad (5.34)$$

Similarly, C is translationally invariant.

The remaining lattice symmetries correspond to the point group of the cubic lattice,¹⁵ which is the octahedral group, denoted as O_h . It is isomorphic to $S_4 \times \mathbb{Z}_2$, where S_4 is associated with orientation-preserving symmetries (rotations) and \mathbb{Z}_2 is associated with the reflection (parity). It is easy to see that the ZX-diagrams of the duality maps $D_{p \leftarrow 1}$ and $D_{1 \leftarrow p}$, and the condensation operator C are invariant under rotations and reflections. So the nontrivial action on D comes from the transformation of the half-translation maps $T_{p \leftarrow 1}$ and $T_{1 \leftarrow p}$.

The parity operator P acts as

$$PT_{\mathbf{a}}P = T_{\mathbf{a}}^\dagger = T_{-\mathbf{a}}, \quad PDP = DT_{1,1,1}^{-1} = D^\dagger, \quad (5.35)$$

where the latter follows from the fact that the half-translation map $T_{p \leftarrow 1}$, associated with the half-translation \mathfrak{t} , transforms into $(T_{1 \leftarrow p})^\dagger = T_{p \leftarrow 1}^{-1}$, associated with \mathfrak{t}^{-1} , under parity $(x, y, z) \mapsto (-x, -y, -z)$. A similar statement holds for the other half-translation map $T_{1 \leftarrow p}$.

Let us consider rotations now. It is well-known that S_4 acts freely and transitively on the space-diagonals of a cube. It follows that, given a rotation R , there is a unique $\boldsymbol{\varepsilon} = (\varepsilon_x, \varepsilon_y, \varepsilon_z) \in \{\pm 1\}^3$ such that $RT_{1,1,1}R^{-1} = T_{\boldsymbol{\varepsilon}}$.¹⁶ We define $D_{\boldsymbol{\varepsilon}} := RDR^{-1}$; in particular, $D_{1,1,1} = D$. Then,

$$D_{\boldsymbol{\varepsilon}}^2 = RD^2R^{-1} = RT_{1,1,1}CR^{-1} = T_{\boldsymbol{\varepsilon}}C, \quad (5.36)$$

where we used the fact that the ZX-diagram of C is rotationally invariant. In fact, $D_{\boldsymbol{\varepsilon}}$ is related to D by a translation,¹⁷

$$D_{\boldsymbol{\varepsilon}} = DT_{\frac{1}{2}(\boldsymbol{\varepsilon}-\mathbf{1})}, \quad (5.37)$$

where $\mathbf{1} = (1, 1, 1)$. In particular, $D_{-1,-1,-1} = D^\dagger$.

Consider the special case where the rotation R fixes the space diagonal along $(1, 1, 1)$ —such

¹⁵Technically, the rotational part of this group exists only when $L_x = L_y = L_z$ or when the lattice is infinite.

¹⁶One can think of $\boldsymbol{\varepsilon}$ as labelling the space-diagonal along that direction. Note that $\boldsymbol{\varepsilon}$ and $-\boldsymbol{\varepsilon}$ label the same space-diagonal.

¹⁷The half translation map $T_{p \leftarrow 1}$ transforms into $T_{p \leftarrow 1}^\boldsymbol{\varepsilon}$ under the rotation R . Here, $T_{p \leftarrow 1}^\boldsymbol{\varepsilon}$ maps the physical qubit on link ℓ to the auxiliary qubit on plaquette $\mathfrak{t}_\boldsymbol{\varepsilon}(\ell)$, where $\mathfrak{t}_\boldsymbol{\varepsilon}(\mathbf{x}) = \mathbf{x} + \frac{1}{2}\boldsymbol{\varepsilon}$ is the half-translation in the $\boldsymbol{\varepsilon}$ direction. The desired relation then follows from the simple observation $T_{p \leftarrow 1}^\boldsymbol{\varepsilon} = T_{p \leftarrow 1}T_{\frac{1}{2}(\boldsymbol{\varepsilon}-\mathbf{1})}$. Similar statements apply to the other half-translation map $T_{1 \leftarrow p}$.

rotations form the S_3 subgroup of S_4 . This can happen in two ways:

1. R is the $2\pi/3$ -rotation about the $(1, 1, 1)$ direction, which generates the \mathbb{Z}_3 subgroup of the stabilizer group S_3 . Then, $RT_{1,1,1}R^{-1} = T_{1,1,1}$ and $RDR^{-1} = D$.
2. R is the π -rotation about $(1, -1, 0)$, $(0, 1, -1)$, or $(-1, 0, 1)$ direction. Then, $RT_{1,1,1}R^{-1} = T_{-1,-1,-1}$ and $RDR^{-1} = D^\dagger$.

Note that D is mapped to D^\dagger by both the parity P , which is an orientation-reversing operation, and the rotation R of the second-type above, which is an orientation-preserving operation. This is the lattice counterpart of the continuum fact that $\mathcal{D}(M)$ is the same as its orientation reversal.

5.5 Action on the toric code ground states

The phase diagram of the lattice \mathbb{Z}_2 gauge theory (4.2) is well understood [97]: the \mathbb{Z}_2 1-form symmetry is spontaneously broken (Higgs phase) for $J > h$, whereas it is preserved (confining phase) for $J < h$. The broken phase is captured by the 3+1d topological \mathbb{Z}_2 gauge theory at low energies. At the self-dual point $J = h$, there is a first order phase transition.

Let us say a few words about the ground states in these phases. In the limit $J \gg h$ (or when $h = 0$), the magnetic flux term dominates. On a cubic lattice with periodic boundary conditions, this leads to $2^3 = 8$ ground states,

$$|\xi\rangle := 2^{(V-1)/2} \prod_{i<j} \eta_{ij}^{\xi_{ij}} \prod_s \left(\frac{1 + G_s}{2} \right) |0 \cdots 0\rangle, \quad (5.38)$$

where $\xi = (\xi_{xy}, \xi_{yz}, \xi_{zx}) \in \{0, 1\}^3$ with ξ_{ij} defined modulo 2. We recognize that $|\xi\rangle$ are the ground states of the 3+1d toric code.¹⁸ On the other hand, in the limit $J \ll h$ (or when $J = 0$), the electric field term dominates, so there is a unique ground state,

$$|+\cdots+\rangle. \quad (5.39)$$

At the self-dual point $J = h$, there are nine ground states in the thermodynamic limit. These ground states are not the above nine states, but are related to them by a finite depth local unitary (FDLU). Incidentally, these eight toric code ground states $|\xi\rangle$ and the product state $|+\cdots+\rangle$ are the exact ground states of the Hamiltonian in (5.46) at $\lambda = 1$ discussed below.

Irrespective of the model, one can ask how the symmetry operators η_{ij} and D act on these ground states. Clearly, the 1-form symmetries η_{ij} permute the toric code ground states among themselves and leave the product state invariant:

$$\prod_{i<j} \eta_{ij}^{\xi'_{ij}} |\xi\rangle = |\xi + \xi'\rangle, \quad \eta_{ij} |+\cdots+\rangle = |+\cdots+\rangle. \quad (5.40)$$

¹⁸Indeed, starting with the Hamiltonian H (4.5), which has the same ground states as \tilde{H} (4.2) for $g > 0$, and setting $h = 0$ gives the Hamiltonian of the 3+1d toric code. The normalization of $|\xi\rangle$ is chosen such that $\langle \xi | \xi' \rangle = \delta_{\xi, \xi'}$.

More interestingly, the non-invertible symmetry exchanges the toric code ground states with the product state:

$$D|\xi\rangle = \frac{1}{\sqrt{2}}|+\cdots+\rangle, \quad D|+\cdots+\rangle = \frac{1}{\sqrt{2}} \sum_{\xi \in \{0,1\}^3} |\xi\rangle. \quad (5.41)$$

We interpret the above equations as the spontaneous breaking of the non-invertible Wegner symmetry D and the 1-form symmetry η . We derive (5.41) using ZX-calculus in Appendix A.3.

The basis in (5.38) and (5.39) corresponds to the ground states in the nine superselection sectors of the model in (5.46) in the thermodynamic limit. Alternatively, for $\zeta = (\zeta_{xy}, \zeta_{yz}, \zeta_{zx}) \in \{0,1\}^3$, we define

$$|\zeta\rangle := \frac{1}{2\sqrt{2}} \sum_{\xi \in \{0,1\}^3} (-1)^{\sum_{i<j} \zeta_{ij} \xi_{ij}} |\xi\rangle. \quad (5.42)$$

Then, the basis that diagonalizes the symmetry operators can be written as¹⁹

$$\begin{aligned} \frac{1}{\sqrt{2}}|+\cdots+\rangle \pm \frac{1}{\sqrt{2}}|\zeta=0\rangle, & \quad D = \pm 2, \quad \eta_{ij} = 1, \\ |\zeta \neq 0\rangle, & \quad D = 0, \quad \eta_{ij} = (-1)^{\zeta_{ij}}. \end{aligned} \quad (5.43)$$

See Appendix A.4 for more discussions on the two bases $|\xi\rangle$ and $|\zeta\rangle$ for the toric code ground states.

Using (5.26), we see that the toric code ground state $|\zeta=0\rangle$ can be obtained by acting the condensation operator on a product state:²⁰

$$|\zeta=0\rangle = \frac{2^{V/2}}{2} C|0\cdots 0\rangle. \quad (5.44)$$

This generalizes the relation $|\text{GHZ}^+\rangle = \frac{1}{\sqrt{2}}(1+\eta)|0\cdots 0\rangle$ in 1+1d. The duality operator D exchanges this toric code ground state $|\zeta=0\rangle$ and the product state $|+\cdots+\rangle$:

$$D|\zeta=0\rangle = 2|+\cdots+\rangle, \quad D|+\cdots+\rangle = 2|\zeta=0\rangle. \quad (5.45)$$

This is the 3+1d analog of the relation (3.36) in 1+1d.

5.6 LSM-type constraint and duality-preserving deformations

Here we argue that, in the thermodynamic limit $L_i \rightarrow \infty$, any Hamiltonian that commutes with the non-invertible operator D cannot be in a trivially gapped phase with a unique ground state without long range entanglement. It is either gapless, gapped with multiple superselection sectors, or gapped with topological order.

¹⁹Comparing with the discussion in Section 3.4, the basis $|\xi\rangle$ is the analog of $|0\cdots 0\rangle, |1\cdots 1\rangle$ in 1+1d, while the basis $|\zeta\rangle$ is the analog of $|\text{GHZ}^\pm\rangle$.

²⁰On the other hand, the state $|\xi=0\rangle$ can be obtained by acting a condensation operator for a 2-form symmetry on the product state $|+\cdots+\rangle$. See Appendix A.4, in particular, (A.28).

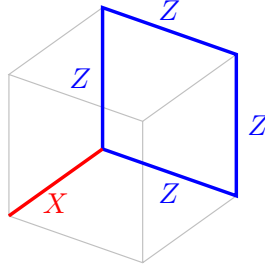


Figure 7: The deformation term in \tilde{H}_λ (5.46). As indicated, the red (blue) links represent the Pauli X (Z) operators on links. We add such a term for every link and plaquette that are orthogonal to each other and meet at a site. For example, each cube contains 24 such terms.

This constraint is reminiscent of the Lieb-Schultz-Mattis (LSM) theorem [98], and is a 3+1d generalization of the constraint for the 1+1d Kramers-Wannier symmetry in [18, 15]. Our lattice argument largely follows from the corresponding theorem in the 3+1d continuum field theory proven in [51], which was interpreted as an 't Hooft anomaly of the non-invertible global symmetry.²¹

Our setup is a 3d spatial cubic lattice with a qubit on each link. We assume that the Gauss law $G_s = \prod_{\ell \ni s} X_\ell = 1$ is enforced strictly as an operator equation on every site, so that the total Hilbert space is the constrained Hilbert space $\tilde{\mathcal{H}}$, which is a subspace of the tensor product Hilbert space \mathcal{H} . We consider a general translationally invariant Hamiltonian \tilde{H} on $\tilde{\mathcal{H}}$ that is invariant under the topological \mathbb{Z}_2 1-form symmetry $\eta(\hat{\Sigma}) = \prod_{\ell \in \hat{\Sigma}} X_\ell$.

We furthermore assume that the Hamiltonian commutes with the non-invertible operator D , i.e., $D\tilde{H} = \tilde{H}D$. Up to a lattice translation, D implements the gauging of $\mathbb{Z}_2^{(1)}$. (See (5.5) and (4.14).) Therefore, any Hamiltonian that commutes with D must be invariant under gauging the $\mathbb{Z}_2^{(1)}$ symmetry.

As a concrete example, consider a one-parameter deformation of the lattice \mathbb{Z}_2 gauge theory Hamiltonian (5.1) [109]:

$$\tilde{H}_\lambda = -J \left(\sum_p \prod_{\ell \in p} Z_\ell + \sum_\ell X_\ell - \frac{\lambda}{8} \sum_{\ell, p: \ell \perp p} X_\ell \prod_{\ell' \in p} Z_{\ell'} \right), \quad (5.46)$$

where $\ell \perp p$ (or $p \perp \ell$) means the link ℓ is orthogonal to the plaquette p and they meet at a site. See Figure 7 for an illustration of this deformation. This deformation is analogous to the deformations $X_{i-1}Z_iZ_{i+1}$ and $Z_{i-1}Z_iX_{i+1}$ in the 1+1d model (3.32) in [80]. For any λ , this deformed Hamiltonian preserves the \mathbb{Z}_2 1-form symmetry and the Wegner duality symmetry D .²² It will be shown in [109] that, when $\lambda = 1$, the deformed model has an exact nine-fold ground state degeneracy even in finite volume.

²¹A non-invertible global symmetry is sometimes said to have an 't Hooft anomaly if it is incompatible with a trivially gapped phase [99, 100, 51] (see also [95, 101–105]). See [106–108] for the relation between this definition of anomalies and the obstruction to gauging.

²²To see this, note that $\ell \perp p \iff \mathfrak{t}(\ell) \perp \mathfrak{t}(p)$.

We are now ready to argue for the main statement. Let us assume that the thermodynamic limit of this Hamiltonian is trivially gapped with no long range entanglement. Then in the low energy limit it must be described by a bosonic invertible field theory for the topological phase protected by a $\mathbb{Z}_2^{(1)}$ global symmetry. However, it was shown in [51] that there is no such $\mathbb{Z}_2^{(1)}$ SPT phase that is invariant under gauging the $\mathbb{Z}_2^{(1)}$ symmetry.²³ This proves that the Hamiltonian cannot be in a trivially gapped phase.

What are the gapped phases that are compatible with the non-invertible Wegner symmetry D? A trivially gapped phase is exchanged with a deconfined \mathbb{Z}_2 gauge theory phase under gauging $\mathbb{Z}_2^{(1)}$, and therefore a first order transition point of these two phases is one such example. This phase is realized at the self-dual point $J = h$ for the lattice \mathbb{Z}_2 gauge theory (4.2), and it has 1+8 superselection sectors on a spatial three-torus in the infinite volume limit. It is also realized in the deformed Hamiltonian (5.46) at $\lambda = 1$, where these nine states are the exact ground states even in finite volume. Finally, in the continuum, this phase is realized by the pure SO(3) Yang-Mills gauge theory with $\mathcal{N} = 1$ supersymmetry [112], where the anomalous R-symmetry is resurrected as a non-invertible symmetry [52].²⁴

There can be more general gapped phases compatible with D, which we leave for future investigations.

6 Non-invertible symmetries based on graphs

In this section, we extend the discussion of non-invertible duality operator to a large class of lattice models based on arbitrary bipartite graphs. We refer to them as *generalized transverse-field Ising models* (generalized TFIM) due to their resemblance to the usual transverse-field Ising model. (See [47, 113–120] for related usages of the term “generalized Ising model”. See also [121] for duality *maps* between different models.) We give the condition under which there is a duality symmetry, and derive the condition for which the duality operator does not mix with spatial symmetry. We also discuss several well-known lattice models as examples of this general model.

²³Generally, a bosonic 3+1d $\mathbb{Z}_N^{(1)}$ SPT phase is labeled by an integer p modulo $2N$ if N is even, and p modulo N if N is odd [110, 48]. Under gauging the $\mathbb{Z}_N^{(1)}$ symmetry, the phase remains invertible if $\gcd(p, N) = 1$. Under this condition, gauging maps $p \rightarrow -1/p$ for even N , and $p \rightarrow -1/4p$ for odd N [51]. In particular, when $N = 2$, the $p = 1$ and $p = 3$ SPT phases are exchanged under gauging $\mathbb{Z}_2^{(1)}$, and there is no bosonic SPT phase invariant under the gauging. In [111], the authors further show that for some values of N , there is no fermionic topological quantum field theory (TQFT) (with a unique local operator) that is invariant under gauging $\mathbb{Z}_N^{(1)}$. However, their result does not exclude the possibility of a bosonic TQFT invariant under gauging $\mathbb{Z}_2^{(1)}$.

²⁴We thank Nathan Seiberg for discussions on this point.

6.1 Hamiltonian of the generalized transverse-field Ising model

We consider an arbitrary tensor product Hilbert space of qubits. Denote the set of all qubits V such that the total Hilbert space is $\mathcal{H} := \bigotimes_{v \in V} \mathbb{C}^2$.²⁵ Note that for the current discussion, we do not need to make any assumption yet about geometric locality.

Consider an additional set \widehat{V} and define a bipartite graph \mathcal{G} on $\widehat{V} \sqcup V$, with edge set $E \subseteq \widehat{V} \times V$. Without loss of generality, we assume that \mathcal{G} is connected. Its adjacency matrix takes the form

$$\begin{pmatrix} 0_{|\widehat{V}| \times |\widehat{V}|} & \sigma_{|\widehat{V}| \times |V|} \\ \sigma_{|V| \times |\widehat{V}|}^\top & 0_{|V| \times |V|} \end{pmatrix}, \quad (6.1)$$

where σ is called the biadjacency matrix,²⁶ given by $\sigma_{\hat{v}v} = 1$ if $(\hat{v}, v) \in E$ and 0 otherwise, and its incidence matrix takes the form

$$\begin{pmatrix} \hat{\tau}_{|\widehat{V}| \times |E|} \\ \tau_{|V| \times |E|} \end{pmatrix}, \quad (6.2)$$

where $\hat{\tau}_{\hat{v}e} = 1$ if e is incident to \hat{v} and 0 otherwise, and τ is defined similarly. Note that

$$\sigma = \hat{\tau} \tau^\top. \quad (6.3)$$

Moreover, the entries in all these matrices are 0 or 1.

We may use σ to construct a generalized transverse-field Ising Hamiltonian as follows. First, we define generalized Ising terms

$$B_{\hat{v}} = \prod_{v \in V} Z_v^{\sigma_{\hat{v}v}}, \quad (6.4)$$

for $\hat{v} \in \widehat{V}$ (i.e., for each row \hat{v} of σ , the positions of the Pauli Z 's are given by the entries in that row). Then, we can define the Hamiltonian

$$H = -J \sum_{\hat{v} \in \widehat{V}} B_{\hat{v}} - h \sum_{v \in V} X_v. \quad (6.5)$$

To summarize, an element of V represents a physical qubit while an element of \widehat{V} represents a generalized Ising interaction term.

The invertible symmetries of this Hamiltonian are \mathbb{Z}_2 symmetries. Let us define the operator

$$\eta_a = \prod_{v \in V} X_v^{a_v}, \quad (6.6)$$

for a vector a with components $a_v \in \{0, 1\}$ and see what choices of a give symmetries of this Hamil-

²⁵Throughout this section, we use V to denote a set of vertices which host physical qubits. This is not to be confused with $V = L_x L_y L_z$, the number of sites on the cubic lattice in Section 5.

²⁶In the quantum information literature, σ and \mathcal{G} are called the parity check matrix and the corresponding Tanner graph, respectively.

tonian. For this, we only need to check whether it commutes with the Ising terms. The commutation of a Z-type and an X-type Pauli operators is $\prod_w Z_w^{b_w} \prod_v X_v^{a_v} = (-1)^{\sum_v a_v b_v} \prod_w Z_w^{b_w} \prod_v X_v^{a_v}$. Therefore, the commutation between $B_{\hat{v}}$ and η_a is $(-1)^{\sum_v \sigma_{\hat{v}v} a_v}$, and we see that η_a is a symmetry of the Hamiltonian exactly when $a \in \ker \sigma$. To conclude, the total invertible symmetry group is $\mathbb{Z}_2^{\dim \ker \sigma}$.

6.2 Spatial symmetries from preserving automorphisms

A spatial symmetry of the generalized TFIM on the bipartite graph \mathcal{G} is associated with a *preserving automorphism* π of \mathcal{G} ,²⁷ which satisfies

$$\sigma_{\pi(\hat{v})\pi(v)} = \sigma_{\hat{v}v} . \quad (6.7)$$

Note that $\pi|_V$ is a permutation of the vertices in V . This spatial symmetry is implemented by a permutation operator T_π that maps the qubit at vertex v to the qubit at vertex $\pi(v)$. In particular,

$$T_\pi X_v T_\pi^{-1} = X_{\pi(v)} , \quad T_\pi Z_v T_\pi^{-1} = Z_{\pi(v)} . \quad (6.8)$$

It follows that

$$T_\pi B_{\hat{v}} T_\pi^{-1} = T_\pi \prod_v Z_v^{\sigma_{\hat{v}v}} T_\pi^{-1} = \prod_v Z_{\pi(v)}^{\sigma_{\hat{v}v}} = \prod_v Z_{\pi(v)}^{\sigma_{\pi(\hat{v})\pi(v)}} = \prod_v Z_v^{\sigma_{\pi(\hat{v})v}} = B_{\pi(\hat{v})} . \quad (6.9)$$

Therefore, the Hamiltonian commutes with T_π , i.e.,

$$T_\pi H = H T_\pi . \quad (6.10)$$

Since the composition of two preserving automorphisms is also a preserving automorphism, we have

$$T_\pi T_{\pi'} = T_{\pi \circ \pi'} . \quad (6.11)$$

The operator T_π acts on η_a as

$$T_\pi \eta_a T_\pi^{-1} = T_\pi \prod_v X_v^{a_v} T_\pi^{-1} = \prod_v X_{\pi(v)}^{a_v} = \prod_v X_v^{a_{\pi^{-1}(v)}} = \eta_{\pi \cdot a} , \quad (6.12)$$

where we defined $(\pi \cdot a)_v = a_{\pi^{-1}(v)}$. As a check, note that $\pi \cdot a \in \ker \sigma$ because $\sum_v \sigma_{\hat{v}v} (\pi \cdot a)_v = \sum_v \sigma_{\pi^{-1}(\hat{v})v} a_v = 0$.

²⁷An *automorphism* α of a graph is a bijection from its vertex-set to itself such that $\alpha(v)$ and $\alpha(w)$ have an edge between them if and only if v and w have an edge between them. For a bipartite graph, an automorphism is said to be *preserving* if it fixes the two parts of the vertex-set, i.e., $\alpha(V) = V$ and $\alpha(\hat{V}) = \hat{V}$, whereas it is said to be *reversing* if it exchanges the two parts of the vertex-set, i.e., $\alpha(V) = \hat{V}$ and $\alpha(\hat{V}) = V$.

6.3 Non-invertible duality operators from reversing automorphisms

Let us now construct a map $D_{\hat{v} \leftarrow v} : \mathcal{H} \rightarrow \hat{\mathcal{H}}$, where $\hat{\mathcal{H}} := \bigotimes_{\hat{v} \in \hat{V}} \mathbb{C}^2$, as a ZX-diagram where we replace vertices of \mathcal{G} with green spiders, place Hadamards on the edges, and add input legs into V and output legs out of \hat{V} . After a color change CC', the ZX-diagram representing this map is given by

$$D_{\hat{v} \leftarrow v} := 2^\kappa \begin{array}{c} v \in V \\ \text{---} \circ \text{---} \\ \vdots \\ \text{---} \circ \text{---} \\ \sigma \\ \text{---} \circ \text{---} \\ \vdots \\ \text{---} \circ \text{---} \\ \hat{v} \in \hat{V} \end{array}, \quad (6.13)$$

where κ is a real number to be fixed later and the middle part of the diagram is understood as follows: for each green dot labelled by $v \in V$ and each red dot labelled by $\hat{v} \in \hat{V}$, the number of wires connecting them is $\sigma_{\hat{v}v}$. One can similarly define the map $D_{v \leftarrow \hat{v}}$, whose ZX-diagram is obtained by flipping the ZX-diagram of $D_{\hat{v} \leftarrow v}$ horizontally, i.e., $D_{v \leftarrow \hat{v}} = (D_{\hat{v} \leftarrow v})^\dagger$.

The map $D_{\hat{v} \leftarrow v}$ implements the gauging of the \mathbb{Z}_2 symmetries generated by η_a 's. (Such a map was studied in [122, 123, 113, 114, 92, 124–126, 115, 127, 128, 116, 82, 84, 129, 130, 119, 121].) Indeed, commuting the Hamiltonian H through $D_{\hat{v} \leftarrow v}$ gives the gauged Hamiltonian \hat{H} , i.e.,

$$D_{\hat{v} \leftarrow v} H = \hat{H} D_{\hat{v} \leftarrow v}, \quad (6.14)$$

where

$$\hat{H} = -h \sum_{v \in V} \hat{B}_v - J \sum_{\hat{v} \in \hat{V}} \hat{X}_{\hat{v}}, \quad \hat{B}_v = \prod_{\hat{v} \in \hat{V}} \hat{Z}_{\hat{v}}^{\sigma_{\hat{v}v}}. \quad (6.15)$$

Evidently, the gauged Hamiltonian \hat{H} is also a generalized TFIM, albeit on a different Hilbert space $\hat{\mathcal{H}}$.

So far we have defined a map between two Hilbert spaces \mathcal{H} and $\hat{\mathcal{H}}$. To turn it into an operator that acts within one Hilbert space, we need to identify these two Hilbert spaces in some way.

More precisely, this is achieved by choosing a *reversing automorphism* ρ of \mathcal{G} ,²⁸ which satisfies

$$\sigma_{\rho(v)\rho(\hat{v})} = \sigma_{\hat{v}v}. \quad (6.16)$$

Define the map $T_{\hat{v} \leftarrow v}^\rho : \mathcal{H} \rightarrow \hat{\mathcal{H}}$ that maps the physical qubit at vertex v to the auxiliary qubit at vertex $\rho(v)$. One can similarly define the map $T_{v \leftarrow \hat{v}}^\rho$. Since ρ is reversing, ρ^2 is preserving, and we have

$$T_{v \leftarrow \hat{v}}^\rho T_{\hat{v} \leftarrow v}^\rho = T_{\rho^2}. \quad (6.17)$$

More generally, we have

$$T_{v \leftarrow \hat{v}}^\rho T_{\hat{v} \leftarrow v}^{\rho'} = T_{\rho \circ \rho'}, \quad (6.18)$$

²⁸Two necessary conditions for the existence of a reversing automorphism are (i) $|V| = |\hat{V}|$ and (ii) the *degree-sequences* of vertices in V and \hat{V} match. However, they are not sufficient—a bipartite graph which satisfies these conditions but does not have a reversing automorphism can be found in [131].

which is well-defined because the composition of two reversing automorphisms is a preserving automorphism. Similarly, we have

$$T_\pi T_{v \leftarrow \hat{v}}^\rho = T_{v \leftarrow \hat{v}}^{\pi \circ \rho}, \quad T_{\hat{v} \leftarrow v}^\rho T_\pi = T_{\hat{v} \leftarrow v}^{\rho \circ \pi}, \quad (6.19)$$

which are well-defined because the composition of a reversing automorphism and a preserving automorphism is a reversing automorphism.

For every reversing automorphism ρ of \mathcal{G} , we define a non-invertible duality operator $D_\rho : \mathcal{H} \rightarrow \mathcal{H}$ as

$$D_\rho := T_{v \leftarrow \hat{v}}^\rho D_{\hat{v} \leftarrow v} = D_{v \leftarrow \hat{v}} T_{\hat{v} \leftarrow v}^\rho, \quad (6.20)$$

where the equality of the two factorizations follows from (6.16). From (6.19), we have

$$T_\pi D_\rho = D_{\pi \circ \rho}, \quad D_\rho T_\pi = D_{\rho \circ \pi}. \quad (6.21)$$

6.4 Action on operators

D_ρ acts on the \mathbb{Z}_2 -symmetric operators as

$$D_\rho X_v = T_{v \leftarrow \hat{v}}^\rho \prod_{\hat{v} \in \hat{V}} \widehat{Z}_{\hat{v}}^{\sigma \hat{v} v} D_{\hat{v} \leftarrow v} = \prod_{\hat{v} \in \hat{V}} Z_{\rho(\hat{v})}^{\sigma \hat{v} v} D_\rho = \prod_{\hat{v} \in \hat{V}} Z_{\rho(\hat{v})}^{\sigma_{\rho(v)} \rho(\hat{v})} D_\rho = B_{\rho(v)} D_\rho, \quad (6.22)$$

and similarly,

$$D_\rho B_{\hat{v}} = X_{\rho(\hat{v})} D_\rho. \quad (6.23)$$

This can be seen easily using ZX-calculus by pushing a red spider with a π phase through a vertex on either side of the ZX-diagram of $D_{\hat{v} \leftarrow v}$. Thus, it is clear that D_ρ commutes with the Hamiltonian when $J = h$. Moreover, we have

$$D_\rho \eta_a = D_\rho \prod_{v \in V} X_v^{a_v} = \prod_{v \in V} B_{\rho(v)}^{a_v} D_\rho = \prod_{v \in V} \prod_{u \in V} Z_u^{\sigma_{\rho(v)} u^{a_v}} D_\rho = \prod_{v \in V} \prod_{u \in V} Z_u^{\sigma_{\rho^{-1}(u)} v^{a_v}} D_\rho = D_\rho. \quad (6.24)$$

where used $a \in \ker \sigma$. Similarly, we have $\eta_a D_\rho = D_\rho$.

6.5 Operator algebra

Let us look at the action of D_ρ^2 on symmetric operators:

$$\begin{aligned} D_\rho^2 X_v &= D_\rho B_{\rho(v)} D_\rho = X_{\rho^2(v)} D_\rho^2, \\ D_\rho^2 B_{\hat{v}} &= D_\rho X_{\rho(\hat{v})} D_\rho = B_{\rho^2(\hat{v})} D_\rho^2. \end{aligned} \quad (6.25)$$

So one might expect that

$$D_\rho^2 \propto T_{\rho^2} \sum_{a \in \ker \sigma} \eta_a. \quad (6.26)$$

Indeed, we verify this using ZX-calculus. First, we have

$$D_\rho^2 = D_{v \leftarrow \hat{v}} T_{\hat{v} \leftarrow v}^\rho D_{v \leftarrow \hat{v}} T_{\hat{v} \leftarrow v}^\rho = D_{v \leftarrow \hat{v}} D_{\hat{v} \leftarrow v} T_{\rho^2} = T_{\rho^2} D_{v \leftarrow \hat{v}} D_{\hat{v} \leftarrow v}. \quad (6.27)$$

Now,

$$D_{v \leftarrow \hat{v}} D_{\hat{v} \leftarrow v} \stackrel{\text{HC,SF}}{\cong} 2^{2\kappa} \begin{array}{c} v \in V \quad \hat{v} \in \hat{V} \quad v' \in V \\ \text{---} \text{---} \text{---} \\ \vdots \quad \sigma \quad \vdots \quad \sigma^\top \quad \vdots \\ \text{---} \text{---} \text{---} \\ \vdots \quad \vdots \quad \vdots \end{array} \stackrel{\text{SF}}{\cong} 2^{2\kappa} \begin{array}{c} \text{---} \text{---} \text{---} \\ \vdots \quad \tau^\top \quad \vdots \quad \tau \quad \vdots \\ \text{---} \text{---} \text{---} \\ v \in V \quad e \in E \quad v' \in V \end{array}, \quad (6.28)$$

where in the second equality, we used (6.3). Now, for each $v \in V$, we apply the generalized bialgebra GB on the following part of the diagram:

$$\begin{array}{c} \vdots \\ \vdots \\ \text{---} \text{---} \text{---} \\ \vdots \quad \vdots \quad \vdots \\ \text{---} \text{---} \text{---} \\ \vdots \quad \vdots \quad \vdots \\ v \text{---} \text{---} v \\ e \in E_v \end{array} \stackrel{\text{GB}}{\cong} \left(\frac{1}{\sqrt{2}} \right)^{d_v-1} \begin{array}{c} \text{---} \text{---} \\ \vdots \quad \vdots \\ \text{---} \text{---} \\ e \in E_v \\ v \text{---} v \end{array}, \quad (6.29)$$

where E_v is the set of edges incident to v and $d_v = |E_v|$ is the degree of the vertex v . Using this and noting that $E = \bigsqcup_{v \in V} E_v$, we get²⁹

$$\begin{aligned} D_{v \leftarrow \hat{v}} D_{\hat{v} \leftarrow v} &= 2^{2\kappa} \left(\frac{1}{\sqrt{2}} \right)^{\sum_{v \in V} (d_v-1)} \begin{array}{c} e \in E \quad \hat{v} \in \hat{V} \\ \text{---} \text{---} \text{---} \\ \vdots \quad \tau^\top \quad \vdots \quad \tau \quad \vdots \\ \text{---} \text{---} \text{---} \\ v \in V \end{array} \\ &= 2^{2\kappa} \left(\frac{1}{\sqrt{2}} \right)^{|E|-|V|} \begin{array}{c} \hat{v} \in \hat{V} \\ \text{---} \text{---} \text{---} \\ \vdots \quad \sigma \quad \vdots \\ \text{---} \text{---} \text{---} \\ v \in V \end{array} =: \mathbf{C}, \end{aligned} \quad (6.30)$$

²⁹The diagram in the first line is well-defined because for each e , there is only one $v \in V$ and one $\hat{v} \in \hat{V}$ that it is incident to. In other words, there are no dangling wires and no junctions of wires at any $e \in E$.

where we used $|E| = \sum_{v \in V} d_v$, and defined the condensation operator C . Therefore, we have

$$D_\rho^2 = T_{\rho^2} C . \quad (6.31)$$

More generally, for two reversing automorphisms ρ and ρ' , one can show that

$$D_\rho D_{\rho'} = T_{\rho \circ \rho'} C . \quad (6.32)$$

Note that D_ρ mixes with the spatial symmetry generated by T_{ρ^2} , generalizing the observation in [14, 15]. In the special case when the reversing automorphism ρ is an *involution*—i.e., $\rho^2 = 1$, where 1 is the identity automorphism—then we see that the duality operator D_ρ does not mix with any spatial symmetry. We will see examples of this below.

We can find the Pauli representation of C as follows. Using (A.1) for all the green dots, we have

$$\begin{aligned} C &= 2^{2\kappa} \left(\frac{1}{\sqrt{2}} \right)^{|E|-|V|} \frac{(\sqrt{2})^{2 \sum_{v \in V} 1}}{(\sqrt{2})^{\sum_{v \in V} (d_v + 1)}} \left(\bigotimes_{\hat{v} \in \hat{V}} \langle 0 |_{\hat{v}} \right) \left[\prod_{v \in V} \left(1 + X_v \prod_{\hat{v} \in \hat{V}} \hat{X}_{\hat{v}}^{\sigma_{\hat{v}v}} \right) \right] \left(\bigotimes_{\hat{v} \in \hat{V}} |0 \rangle_{\hat{v}} \right) \\ &= \frac{2^{2\kappa}}{2^{|E|-|V|}} \sum_{a \in \{0,1\}^{|V|}} \prod_{v \in V} X_v^{a_v} \prod_{\hat{v} \in \hat{V}} \delta_{\sum_{v \in V} \sigma_{\hat{v}v} a_v, 0} \\ &= \frac{2^{2\kappa}}{2^{|E|-|V|}} \sum_{a \in \ker \sigma} \eta_a , \end{aligned} \quad (6.33)$$

and hence,

$$D_\rho^2 = \frac{2^{2\kappa}}{2^{|E|-|V|}} T_{\rho^2} \sum_{a \in \ker \sigma} \eta_a . \quad (6.34)$$

It follows that

$$D_\rho C = C D_\rho = \frac{2^{2\kappa} \cdot 2^{\dim \ker \sigma}}{2^{|E|-|V|}} D_\rho . \quad (6.35)$$

We will say more about the choice of κ in the examples below. It turns out that, in all the examples that are translationally invariant, there is a natural choice of κ such that all extensive factors cancel in the fusion of D and C . The remaining coefficient is precisely the fusion coefficient expected from the continuum.

The following is a summary of the algebra of all symmetry operators:

$$\begin{aligned} \eta_a \eta_{a'} &= \eta_{a+a'} , & T_\pi T_{\pi'} &= T_{\pi \circ \pi'} , & T_\pi \eta_a &= \eta_{\pi \cdot a} T_\pi , \\ D_\rho \eta_a &= \eta_a D_\rho = D_\rho , & T_\pi D_\rho &= D_{\pi \circ \rho} , & D_\rho T_\pi &= D_{\rho \circ \pi} , \\ D_\rho D_{\rho'} &= T_{\rho \circ \rho'} C , & C &= \frac{2^{2\kappa}}{2^{|E|-|V|}} \sum_{a \in \ker \sigma} \eta_a , \end{aligned} \quad (6.36)$$

where $a, a' \in \ker \sigma$, π, π' are preserving automorphisms, $(\pi \cdot a)_v = a_{\pi^{-1}(v)}$, and ρ, ρ' are reversing automorphisms. The relation between the symmetries of the Hamiltonian H and the properties of

Symmetry	Graph-theoretic property	Fusion rule
Internal \mathbb{Z}_2 's (η_a)	$a \in \ker \sigma$	$\eta_a \eta_{a'} = \eta_{a+a'}$
Spatial (T_π)	Preserving automorphism (π)	$T_\pi T_{\pi'} = T_{\pi \circ \pi'}$
Duality (D_ρ)	Reversing automorphism (ρ)	$D_\rho D_{\rho'} \sim T_{\rho \circ \rho'} \sum_{a \in \ker \sigma} \eta_a$

Table 2: The one-one correspondence between the symmetries of the generalized TFIM and the properties of the associated bipartite graph. When ρ is a reversing involution, i.e., $\rho^2 = 1$, then D_ρ does not mix with spatial symmetries.

the bipartite graph \mathcal{G} are summarized in Table 2.

6.6 Examples

6.6.1 1+1d Ising model

In this case, V is the set of L sites on a periodic chain and \widehat{V} is the set of links. We use an integer i to label a site and a half-integer $i + \frac{1}{2}$ to label the link between sites i and $i + 1$. The Hamiltonian is

$$H = -J \sum_i Z_i Z_{i+1} - h \sum_i X_i . \quad (6.37)$$

The associated bipartite graph is shown in Figure 8(a). Its biadjacency matrix is given by

$$\sigma_{i(j+\frac{1}{2})} = \delta_{i,j} + \delta_{i,j+1} . \quad (6.38)$$

The reversing automorphism ρ , shown as blue dashed arrow in Figure 8(a), corresponds to a half-translation. This leads to the KW duality operator D , which mixes with lattice translation as in (3.17). Since $|V| = L$, $|E| = 2L$, and $\dim \ker \sigma = 1$, we choose $\kappa = L/2$ to cancel all the extensive factors. This gives $DC = CD = 2D$, which is precisely what we obtained in Section 3.3.

The half-translation ρ and all its odd powers are not the only reversing automorphisms of the bipartite graph in Figure 8(a). In fact, there is a reversing involution ρ' , shown as red arrow in Figure 8(a), that corresponds to a reflection. This leads to a duality operator $D' = DP$ that does not mix with lattice translation. (Here, P is the parity operator that maps the qubit at i to the qubit at $-i$.) Indeed, using $DP = PD^\dagger$ and $TP = PT^\dagger$ (it is easy to see this using ZX-calculus), we have

$$(D')^2 = DPDP = DD^\dagger = 1 + \eta . \quad (6.39)$$

While D' commutes with η , it does not commute with T :

$$D'T = T^\dagger D' . \quad (6.40)$$

Moreover, D' maps local symmetric operators around the site i to those around the site $-i$. There-

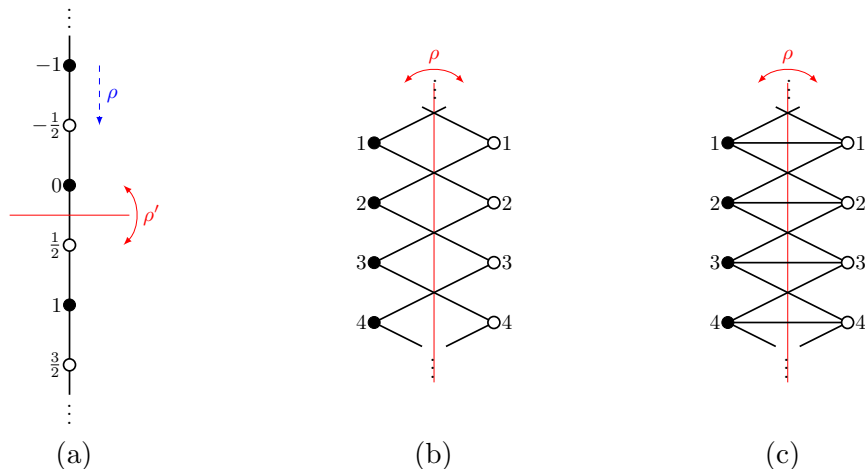


Figure 8: The bipartite graphs for the 1+1d examples: (a) the transverse-field Ising model (6.37), (b) the Ashkin-Teller model at $\lambda = 0$ (6.44), and (c) the three-spin Ising model (6.49). The vertex-sets V and \widehat{V} correspond to the solid and hollow vertices, respectively. The blue (dashed) arrow indicates a reversing automorphism that is not an involution and the red arrows indicate reversing involutions.

fore, we refer to D' as a *non-invertible parity (or reflection) operator*. (See [52,101] for non-invertible parity and time-reversal symmetries in continuum field theory.)

6.6.2 3+1d lattice \mathbb{Z}_2 gauge theory

In this case, V is the set of links on an $L_x \times L_y \times L_z$ periodic cubic lattice and \widehat{V} is the set of plaquettes. We use ℓ to label a link and p to label a plaquette. The Hamiltonian is

$$H = -J \sum_p \prod_{\ell \in p} Z_\ell - h \sum_\ell X_\ell . \quad (6.41)$$

Note that we do not impose Gauss law here, or equivalently, we set $g = 0$ in (4.5). The biadjacency matrix in this case is given by

$$\sigma_{\ell p} = \sum_{\ell' \in p} \delta_{\ell, \ell'} . \quad (6.42)$$

Since $|V| = 3L_x L_y L_z$, $|E| = 12L_x L_y L_z$, and $\dim \ker \sigma = L_x L_y L_z + 2$, we choose $\kappa = 4L_x L_y L_z$ to cancel all the extensive factors. This gives $DC = CD = 4D$, which is precisely what we obtained in (5.29).

There is a reversing automorphism given by the half-translation \mathfrak{t} in the $(1, 1, 1)$ direction. The leads to the Wegner duality operator D (5.10), which mixes with the lattice translation $T_{1,1,1}$.

There is also a reversing involution given by parity, or equivalently, a reflection followed by a π -rotation. This gives a duality operator $D' = DP$ that does not mix with lattice translation.

(Here, P is the usual parity operator that maps the qubit at link ℓ to the qubit at link $\mathfrak{p}(\ell)$, where

$$\mathfrak{p}(x, y, z) = (-x, -y, -z) \pmod{(L_x, L_y, L_z)} , \quad (6.43)$$

is the parity map on the lattice.) Since D' maps local symmetric operators around the link ℓ to those around the link $\mathfrak{p}(\ell)$, we refer to it as a non-invertible parity operator.

6.6.3 1+1d Ashkin-Teller model

The Hamiltonian is [132–136]

$$\begin{aligned} H = & -J \sum_i (Z_{2i-1}Z_{2i+1} + Z_{2i}Z_{2i+2} + \lambda Z_{2i-1}Z_{2i}Z_{2i+1}Z_{2i+2}) \\ & - h \sum_i (X_{2i} + X_{2i+1} + \lambda X_{2i}X_{2i+1}) . \end{aligned} \quad (6.44)$$

Assuming $L \in 2\mathbb{Z}$, this model has two \mathbb{Z}_2 symmetries generated by

$$\eta_{\text{odd}} = \prod_i X_{2i-1} , \quad \eta_{\text{even}} = \prod_i X_{2i} . \quad (6.45)$$

When $J = h$, it is self-dual under the exchange

$$Z_{2i-1}Z_{2i+1} \longleftrightarrow X_{2i} , \quad Z_{2i}Z_{2i+2} \longleftrightarrow X_{2i+1} . \quad (6.46)$$

When $\lambda = 0$, this model is equivalent to two copies of the TFIM on the odd and even sites, respectively.³⁰ The phase diagram of the quantum Ashkin-Teller (AT) model is well-studied [135, 139]. Along $J = h$, for a range of λ , there is a critical line with continuously varying critical exponents described by the orbifold branch of the $c = 1$ CFT. In particular, at $J = h$ and $\lambda = 0$, the critical point is described by the Ising² point on the orbifold branch of the $c = 1$ CFT, as expected from the above equivalence. Related discussions can be found in [140, 44].

In this case, V and \widehat{V} are both the set of all sites, labelled by an integer i . The corresponding bipartite graph is shown in Figure 8(b). Its biadjacency matrix is given by

$$\sigma_{ij} = \delta_{i,j-1} + \delta_{i,j+1} . \quad (6.47)$$

The generalized TFIM associated with this graph corresponds to the $\lambda = 0$ case.

There is a reversing involution ρ , shown as red arrow in Figure 8(b), that flips the graph about the red vertical line. Therefore, the duality operator D which implements the above exchange does

³⁰It is also equivalent to the \mathbb{Z}_2 dipole Ising model [137], so one can interpret this duality as the dipole KW duality [46, 138].

not mix with lattice translation:

$$D^2 = C = (1 + \eta_{\text{odd}})(1 + \eta_{\text{even}}) . \quad (6.48)$$

Here, since $|V| = L$, $|E| = 2L$, and $\dim \ker \sigma = 2$, we chose $\kappa = L/2$ to cancel all the extensive factors, and hence, $DC = CD = 4D$.

We remark that the operators D , η_{odd} , and η_{even} together form the fusion category $\text{Rep}(D_8)$. Apart from the AT model, there are also other Hamiltonians which enjoy this symmetry, such as the 1+1d cluster Hamiltonian [27]. This non-invertible symmetry in the continuum $c = 1$ orbifold CFT was discussed in [141, 108, 142, 143].

6.6.4 1+1d three-spin Ising model

The Hamiltonian is

$$H = -J \sum_i Z_{i-1} Z_i Z_{i+1} - h \sum_i X_i . \quad (6.49)$$

Assuming $L \in 3\mathbb{Z}$, this model has two \mathbb{Z}_2 symmetries generated by

$$\eta_1 = \prod_{i \notin 3\mathbb{Z}+1} X_i , \quad \eta_2 = \prod_{i \notin 3\mathbb{Z}+2} X_i . \quad (6.50)$$

When $J = h$, it is self-dual under the exchange

$$Z_{i-1} Z_i Z_{i+1} \rightsquigarrow X_i . \quad (6.51)$$

The three-spin Ising model, as well as the duality under the Kramers-Wannier action, has been pointed out in [144–146], as well as recently constructed as a non-invertible symmetry operator [25]. The Hamiltonian at $J = h$ has been studied numerically where the central charge was found to be approximately 1, and the value of the critical exponents suggests that it lies on the orbifold branch of the $c = 1$ CFT moduli space [147–150].

In this case, V and \widehat{V} are both the set of all sites, labelled by an integer i . The corresponding bipartite graph is shown in Figure 8(c). Its biadjacency matrix is given by

$$\sigma_{ij} = \delta_{i,j-1} + \delta_{i,j} + \delta_{i,j+1} . \quad (6.52)$$

There is a reversing involution ρ , shown as red arrow in Figure 8(c), that flips the graph about the red vertical line. Therefore, the duality operator D which implements the above exchange does not mix with lattice translation:

$$D^2 = C = (1 + \eta_1)(1 + \eta_2) . \quad (6.53)$$

Here, since $|V| = L$, $|E| = 3L$, and $\dim \ker \sigma = 2$, we chose $\kappa = L$ to cancel all the extensive factors, and hence, $DC = CD = 4D$. These symmetries form a $\text{Rep}(D_8)$ fusion category.

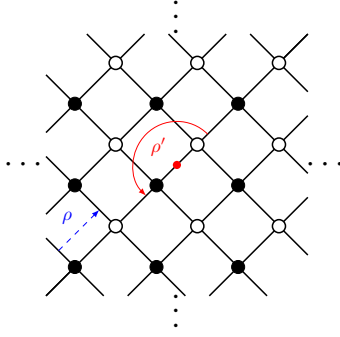


Figure 9: The bipartite graphs for the 2+1d plaquette Ising model (6.54). The vertex-sets V and \widehat{V} correspond to the solid and hollow vertices, respectively. The blue (dashed) arrow indicates a reversing automorphism that is not an involution, whereas the red arrow indicates a reversing involution.

6.6.5 2+1d plaquette Ising model

Consider a 2d $L_x \times L_y$ periodic square lattice with a qubit on each site labelled by (i, j) . The Hamiltonian is

$$H = -J \sum_{i,j} Z_{i,j} Z_{i+1,j} Z_{i,j+1} Z_{i+1,j+1} - h \sum_{i,j} X_{i,j} . \quad (6.54)$$

This model has a \mathbb{Z}_2 subsystem symmetry generated by

$$\eta_i^x = \prod_j X_{i,j} , \quad \eta_j^y = \prod_i X_{i,j} . \quad (6.55)$$

They satisfy the constraint $\prod_i \eta_i^x = \prod_j \eta_j^y$ so there are only $L_x + L_y - 1$ independent generators. When $J = h$, this model is self-dual under the map

$$X_{i,j} \rightsquigarrow Z_{i,j} Z_{i+1,j} Z_{i,j+1} Z_{i+1,j+1} \rightsquigarrow X_{i+1,j+1} , \quad (6.56)$$

which already hints at the duality operator mixing with lattice translation in the $(1, 1)$ direction. This duality was studied in [40, 42, 43].

In this case, V is the set of all sites and \widehat{V} is the set of all plaquettes. We use (i, j) to label a site and $(i + \frac{1}{2}, j + \frac{1}{2})$ to label a plaquette bounded by the sites (i, j) , $(i + 1, j)$, $(i, j + 1)$, and $(i + 1, j + 1)$. The corresponding bipartite graph is shown in Figure 9. Its biadjacency matrix is given by

$$\sigma_{(i,j)(i'+\frac{1}{2},j'+\frac{1}{2})} = \delta_{i,i'} \delta_{j,j'} + \delta_{i,i'+1} \delta_{j,j'} + \delta_{i,i'} \delta_{j,j'+1} + \delta_{i,i'+1} \delta_{j,j'+1} . \quad (6.57)$$

The reversing automorphism ρ , shown as blue dashed arrow in Figure 9, corresponds to the half-translation in $(1, 1)$ direction. It leads to the subsystem KW duality operator D , which mixes

with the lattice translation in the $(1, 1)$ direction as follows:

$$\mathbf{D}^2 = T_{1,1}\mathbf{C}, \quad \text{where} \quad \mathbf{C} = \frac{1}{2} \prod_i (1 + \eta_i^x) \prod_j (1 + \eta_j^y). \quad (6.58)$$

Since $|V| = L_x L_y$, $|E| = 4L_x L_y$, and $\dim \ker \sigma = L_x + L_y - 1$, we choose $\kappa = 3L_x L_y / 2$ to cancel all the extensive factors. This gives $\mathbf{DC} = \mathbf{CD} = 2^{L_x + L_y - 1} \mathbf{D}$.

There is also a reversing involution ρ' , shown as red arrow in Figure 9, given by a π -rotation about the red point. The corresponding duality operator $\mathbf{D}' = \mathbf{D}P$ does not mix with lattice translation. (Here, P is the usual parity operator that maps the qubit at site (i, j) to the qubit at site $(-i, -j)$. Note that P generates a π -rotation in the spatial plane, which is orientation preserving.) We refer to it as a non-invertible parity operator because it maps local symmetric operators around (i, j) to those around $(-i, -j)$.

6.6.6 Tensor product models

A bipartite graph \mathcal{G} has a reversing involution if and only if it is of the form $\mathcal{G}_0 \times K_2$ [151],³¹ where \mathcal{G}_0 is a graph on $|V|$ vertices and K_2 is the complete graph on two vertices (i.e., a “dumbbell”). (Given a reversing involution ρ of \mathcal{G} , we can construct the graph \mathcal{G}_0 as follows: its vertex set is V and there is an edge between v and w if and only if $\sigma_{\rho(v)w} = 1$. This definition is symmetric in v and w because $\sigma_{\rho(v)w} = \sigma_{\rho(w)v}$. Conversely, the map $\rho : (v_0, \epsilon) \mapsto (v_0, 1 - \epsilon)$, where $\epsilon = 0, 1$ labels the vertices of K_2 , gives a reversing involution of $\mathcal{G}_0 \times K_2$.)

All the examples above have reversing involutions so they fall into this category. Below, we consider a special case of this type which leads to a tensor product of decoupled generalized TFIMs.

Consider the case where \mathcal{G}_0 is itself a bipartite graph with vertex-set $\widehat{V}_0 \sqcup V_0$ and edge-set E_0 . Let $\bar{\mathcal{G}}_0$ be the bipartite graph obtained by exchanging the two parts of \mathcal{G}_0 , i.e., $\bar{V}_0 = \widehat{V}_0$ and $\widehat{\bar{V}}_0 = V_0$. Let H_0 be the Hamiltonian of the generalized TFIM based on \mathcal{G}_0 . It is easy to see that the Hamiltonian \bar{H}_0 of the generalized TFIM based on $\bar{\mathcal{G}}_0$ corresponds to the gauged Hamiltonian \widehat{H}_0 (6.15).

Now, the bipartite graph $\mathcal{G} := \mathcal{G}_0 \times K_2$ is canonically isomorphic to the disjoint union of \mathcal{G}_0 and $\bar{\mathcal{G}}_0$, denoted as $\mathcal{G}_0 + \bar{\mathcal{G}}_0$.³² Therefore, the generalized TFIM based on \mathcal{G} is the tensor product

³¹Given two graphs \mathcal{G}_1 and \mathcal{G}_2 , the *tensor (Kronecker) product* $\mathcal{G}_1 \times \mathcal{G}_2$ is defined as the graph with vertex set $V(\mathcal{G}_1) \times V(\mathcal{G}_2)$ such that there is an edge between (v_1, v_2) and (w_1, w_2) if and only if there is an edge between v_i and w_i in \mathcal{G}_i for $i = 1, 2$. The name is inspired by the fact that the adjacency matrix of $\mathcal{G}_1 \times \mathcal{G}_2$ is the tensor (Kronecker) product of the adjacency matrices of \mathcal{G}_1 and \mathcal{G}_2 .

³²An *isomorphism* ϕ from \mathcal{G}_1 to \mathcal{G}_2 is a bijective map $\phi : V(\mathcal{G}_1) \rightarrow V(\mathcal{G}_2)$ such that v_1 and w_1 have an edge between them if and only if $\phi(v_1)$ and $\phi(w_1)$ have an edge between them. Disjoint union of graphs $\mathcal{G}_0 + \bar{\mathcal{G}}_0$ is also known as *graph sum*, which explains this notation. The canonical isomorphism from $\mathcal{G}_0 + \bar{\mathcal{G}}_0$ to \mathcal{G} is given by the obvious inclusions:

$$\begin{aligned} V_0 &\hookrightarrow V_0 \times \{0\}, & \bar{V}_0 = \widehat{V}_0 &\hookrightarrow \widehat{V}_0 \times \{0\}, \\ \widehat{V}_0 &\hookrightarrow \widehat{V}_0 \times \{1\}, & \widehat{\bar{V}}_0 = V_0 &\hookrightarrow V_0 \times \{1\}. \end{aligned} \quad (6.59)$$

of the generalized TFIMs based on \mathcal{G}_0 and $\bar{\mathcal{G}}_0$. In other words, it is the product of a generalized TFIM and its gauged version. More concretely, the total Hilbert space is $\mathcal{H} = \mathcal{H}_0 \otimes \bar{\mathcal{H}}_0$, and the Hamiltonian is

$$H = H_0 + \bar{H}_0 . \quad (6.60)$$

As explained above, $\mathcal{G} = \mathcal{G}_0 \times K_2$ has a reversing involution, and here, it exchanges the two components \mathcal{G}_0 and $\bar{\mathcal{G}}_0$. So there is a duality symmetry that swaps the two Hamiltonians H_0 and \bar{H}_0 in H . The corresponding *non-invertible swap operator* D does not mix with any spatial symmetry; it satisfies

$$D^2 = C = C_0 \bar{C}_0 , \quad (6.61)$$

where C_0 and \bar{C}_0 are the condensation operators of the generalized TFIMs based on \mathcal{G}_0 and $\bar{\mathcal{G}}_0$, respectively.³³

The continuum field theory analog of this model is clear [44, 45, 152]. Let \mathcal{Q}_0 be a general quantum field theory (QFT) with a non-anomalous, generalized symmetry G_0 . Then the tensor product QFT $\mathcal{Q}_0 \times \mathcal{Q}_0/G_0$ has a non-invertible swap symmetry since it is invariant under gauging $G_0 \times \hat{G}_0$, where \hat{G}_0 is the dual symmetry of G_0 .

An example of this type is the Ashkin-Teller model of Section 6.6.3 with $J = h$ and $\lambda = 0$. In this case, the bipartite graphs \mathcal{G}_0 and $\bar{\mathcal{G}}_0$ correspond to the Ising models on even and odd sublattices, respectively. One can also see from Figure 8(b) that there are two connected components, each of which is isomorphic to the bipartite graph in Figure 8(a).

Here is another example in 2+1d that was the focus of [44]. Consider a periodic $L_x \times L_y$ square lattice with qubits on sites and links, labelled by s and ℓ , respectively. The Hamiltonian is

$$H = -J \sum_{\ell} \prod_{s \in \ell} Z_s - h \sum_s X_s - \bar{J} \sum_s \prod_{\ell \ni s} \bar{Z}_{\ell} - \bar{h} \sum_{\ell} \bar{X}_{\ell} . \quad (6.62)$$

One can recognize the first two terms as the Hamiltonian of the 2+1d Ising model on the original lattice and the last two terms as the Hamiltonian of the 2+1d lattice \mathbb{Z}_2 gauge theory on the dual lattice (albeit without the Gauss law constraint). Therefore, it has a $\mathbb{Z}_2^{(0)} \times \mathbb{Z}_2^{(1)}$ symmetry generated by

$$\eta_0 = \prod_s X_s , \quad \bar{\eta}_0(\gamma) = \prod_{\ell \in \gamma} \bar{X}_{\ell} , \quad (6.63)$$

respectively, where γ is a curve along the links of the original lattice. This model also has a non-invertible swap symmetry that exchanges

$$X_s \longleftrightarrow \prod_{\ell \ni s} \bar{Z}_{\ell} , \quad \prod_{s \in \ell} Z_s \longleftrightarrow \bar{X}_{\ell} , \quad (6.64)$$

when $J = \bar{h}$ and $\bar{J} = h$. The corresponding non-invertible swap operator D does not mix with

³³While \mathcal{G}_0 does not necessarily have a duality symmetry, it always has a condensation operator C_0 , which is simply the sum of all the \mathbb{Z}_2 symmetry operators up to a normalization.

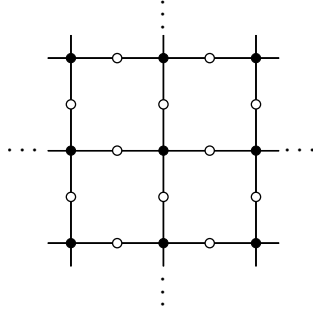


Figure 10: The bipartite graph \mathcal{G}_0 for the 2+1d Ising model. The vertex-sets V_0 and \widehat{V}_0 correspond to the solid and hollow vertices, respectively. The bipartite graph $\bar{\mathcal{G}}_0$ is obtained by replacing solid (hollow) vertices with hollow (solid) vertices.

lattice translation; it satisfies

$$D^2 = C = C_0 \bar{C}_0, \quad DC = CD = 4D, \quad (6.65)$$

where

$$C_0 = 1 + \eta_0, \quad \bar{C}_0 = \frac{1}{2A} \sum_{\gamma} \bar{\eta}_0(\gamma), \quad (6.66)$$

and $A = L_x L_y$.

This example fits into the above model: the vertex-sets V_0 and \widehat{V}_0 are the sites and links, respectively, and there is an edge between s and ℓ if and only if $s \in \ell$. The resulting bipartite graph \mathcal{G}_0 is shown in Figure 10. The generalized TFIM based on \mathcal{G}_0 is the 2+1d Ising model, whereas the one based on $\bar{\mathcal{G}}_0$ is the 2+1d lattice \mathbb{Z}_2 gauge theory. The duality operator associated with the reversing involution of $\mathcal{G} = \mathcal{G}_0 \times K_2 \cong \mathcal{G}_0 + \bar{\mathcal{G}}_0$ is precisely the non-invertible swap operator D . As an aside, note that $|\widehat{V}_0| = 2|V_0|$, so there is no duality symmetry in the 2+1d Ising model or the 2+1d lattice \mathbb{Z}_2 gauge theory separately.

To complete the example, we note that $|V| = |V_0| + |\widehat{V}_0| = 3A$, $|E| = 2|E_0| = 8A$, and $\dim \ker \sigma = \dim \ker \sigma_0 + \dim \ker \bar{\sigma}_0 = 1 + (A + 1) = A + 2$. Therefore, choosing $\kappa = 2A$ to cancel all the extensive factors, we get $DC = CD = 4D$, which agrees with the coefficient above.

6.6.7 On mixing with spatial symmetries

In all the examples above, the bipartite graph has a reversing involution, so there is a duality operator that does not involve a nontrivial permutation of the qubits. In fact, in any $(d + 1)$ -dimensional self-dual generalized TFIM with translation symmetry, there exists a duality operator that does not mix with translations. (For instance, the non-invertible parity operator D' in the 1+1d Ising model.) Therefore, to find models where the duality operator necessarily mixes with a nontrivial permutation of the qubits, one must look beyond models with translation symmetry.

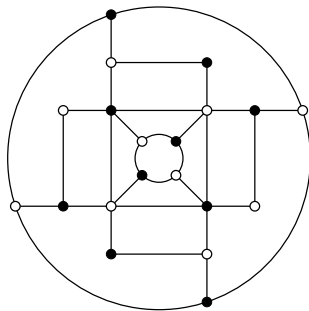


Figure 11: A bipartite graph with a reversing automorphism (90° rotation) but no reversing involution.

As an example, consider the bipartite graph shown in Figure 11.³⁴ It has a reversing automorphism given by a 90° rotation of the graph, but it does not have a reversing involution. So the generalized TFIM based on this graph has a duality symmetry that necessarily mixes with a nontrivial permutation of the qubits. Moreover, the duality operator is non-invertible because $\ker \sigma \neq 0$.

7 Discussions and Outlook

In this work, we used ZX-diagrams to present non-invertible duality operators in many Hamiltonian lattice models, including the Kramers-Wannier operator in the 1+1d Ising model, the Wegner operator in the 3+1d \mathbb{Z}_2 lattice gauge theory, and those in the generalized TFIMs based on graphs. In addition to the duality operator, we also provided graphical presentations for the condensation operators. Their non-invertible algebra was computed using ZX-calculus.

In the generalized TFIM based on a bipartite graph \mathcal{G} , we construct a non-invertible operator D_ρ associated with every reversing automorphism ρ of \mathcal{G} . In the special case when ρ is a reversing involution (i.e., if $\rho^2 = 1$), D_ρ does not mix with spatial symmetries. This is summarized in Table 2.

There are several future directions:

- The generalization to lattice models of n -dimensional qubits with $n > 2$ is particularly interesting since the 't Hooft anomaly of the non-invertible symmetry may depend on n in a nontrivial way, such as in [51]. To this end, one can use an extension of ZX-calculus to qubits, which is known to be universal [153, 154], and also recently shown to be complete [155].
- In this work, we focused on the *operators* implementing the non-invertible symmetry. It is important to extend the discussion of [156, 157, 15] to study the corresponding *defects*, which involve local modifications of the Hamiltonian.

³⁴PG would like to thank Richard Hammack for pointing out a related graph.

- It would be interesting to find the diagrammatic presentation for SPT states protected by (non-anomalous) non-invertible symmetries, generalizing the results of [24].
- Recently, there has been a growing interest in the Kennedy-Tasaki transformation [158, 159, 83, 42, 27, 44, 33], which is a twisted version of the Kramers-Wannier transformation. In the continuum, it corresponds to gauging with a discrete torsion. It is natural consider extending our tensor network presentation to such maps.
- What is the phase diagram for the duality-preserving deformed model in (5.46) in 3+1d? Both the points $\lambda = 0$ and $\lambda = 1$ correspond to a first-order transition between the toric code phase and the product state, and it is plausible that there is no phase transition in between these two values of λ . This is unlike the situation for the analogous 1+1d model in (3.32) where the $\lambda = 0$ point is the Ising CFT while the $\lambda = 1$ point is gapped, and there has to be a nontrivial phase transition in between [80].

Acknowledgements

We are grateful to Clay Córdova, Paul Fendley, Po-Shen Hsin, Ho Tat Lam, Abhinav Prem, Nathan Seiberg, Ruben Verresen, Carolyn Zhang for stimulating discussions. We thank Nathan Seiberg for comments on the draft. SHS thanks Yichul Choi, Yaman Sanghavi, and Yunqin Zheng for collaborations on a related project about non-invertible symmetries in 2+1d lattice gauge theory coupled to Ising matter [44]. PG thanks Tzu-Chen Huang for collaborations on a related project about Wegner duality-preserving deformations of the 3+1d lattice \mathbb{Z}_2 gauge theory [109]. We also thank the authors of [138], which discusses non-invertible symmetries associated with gauging modulated symmetries in 1+1d, for coordinated submissions. The work of PG was supported by the Simons Collaboration on Global Categorical Symmetries. The work of SHS was supported in part by NSF grant PHY-2210182. The work of NT was supported by the Walter Burke Institute for Theoretical Physics at Caltech. This work was initiated at the Aspen Center for Physics during the workshops “Traversing the Particle Physics Peaks: Phenomenology to Formal” and “New Frontiers for Quantum Dynamics” in 2023, which are supported by National Science Foundation grant PHY-2210452. The authors of this paper were ordered alphabetically.

A ZX-calculus for the duality and condensation operators

In this appendix, we provide more details of the ZX-calculus presentation of the duality and condensation operators in the 3+1d lattice \mathbb{Z}_2 gauge theory.

A.1 Condensation operator

Below we show that the two expressions (5.23) and (5.27) for the condensation operator are equivalent.

First, recall that

$$\begin{array}{c} \textcircled{m\pi} \\ \diagdown \quad \diagup \\ 1 \quad \quad \quad 1 \\ \vdots \\ n \quad \quad \quad n \end{array} = \frac{1}{2^{n/2}} [1 + (-1)^m X_1 \cdots X_n] , \quad (\text{A.1})$$

which follows from the discussion below (3.23). Using this identity for each green dot on the link in the ZX-diagram (5.27) of \mathcal{C} , we can write

$$\mathcal{C} \stackrel{\text{SF}}{=} 2^{7V/2} \begin{array}{c} \text{Diagram with red and green dots on links} \\ \ell_x, \ell_y, \ell_z \text{ labels} \end{array} = \frac{2^{7V/2} \cdot 2^{3V}}{2^{15V/2}} \left(\bigotimes_p \langle 0|_p \right) \left[\prod_\ell \left(1 + X_\ell \prod_{p \ni \ell} \widehat{X}_p \right) \right] \left(\bigotimes_p |0\rangle_p \right) , \quad (\text{A.2})$$

where we put a hat on the auxiliary Pauli operator \widehat{X}_p to distinguish it from the physical Pauli operator X_ℓ . Expanding the operator in the middle, we get

$$\mathcal{C} = \frac{1}{2^V} \sum_{\{m_\ell=0,1\}} \prod_\ell X_\ell^{m_\ell} \prod_p \delta_{(dm)_p,0} = \frac{1}{2^V} \sum_{\widehat{\Sigma}} \eta(\widehat{\Sigma}) , \quad (\text{A.3})$$

where, in the third line, $\delta_{a,b}$ is the Kronecker delta function modulo 2, i.e., $\delta_{a,b} = 1$ if $a - b = 0 \pmod 2$ and 0 if $a - b = 1 \pmod 2$. This is precisely the expression for \mathcal{C} in (5.23).

A.2 Duality operator

Here we derive the operator algebra involving \mathcal{D} using ZX-calculus. We start with (5.20), or equivalently, (5.28):

$$\mathcal{D}^2 = \mathcal{C} T_{1,1,1} . \quad (\text{A.4})$$

First, using (5.10), (5.12), and (5.11), we have

$$\mathcal{D}^2 = \mathcal{D}_{l \leftarrow p} T_{p \leftarrow l} \mathcal{D}_{l \leftarrow p} T_{p \leftarrow l} = \mathcal{D}_{l \leftarrow p} \mathcal{D}_{p \leftarrow l} T_{l \leftarrow p} T_{p \leftarrow l} = \mathcal{D}_{l \leftarrow p} \mathcal{D}_{p \leftarrow l} T_{1,1,1} . \quad (\text{A.5})$$

The product $D_{1\leftarrow p}D_{p\leftarrow 1}$ can be computed as follows. We have

$$D_{1\leftarrow p}D_{p\leftarrow 1} = 2^{8V} \cdot \text{Diagram} \quad (\text{A.6})$$

Using color change CC and spider fusion SF, we can simplify this diagram to

$$D_{1\leftarrow p}D_{p\leftarrow 1} = 2^{8V} \cdot \text{Diagram} \quad (\text{A.7})$$

Now, we use the generalized bialgebra GB to simplify it further to

$$D_{1\leftarrow p}D_{p\leftarrow 1} = \frac{2^{8V}}{\underbrace{2^{9V/2}}_{2^{7V/2}}} \cdot \text{Diagram} = C \quad (\text{A.8})$$

It follows that $D^2 = CT_{1,1,1}$.

It is also instructive to compute DC using ZX-calculus. We have

$$D_{p \leftarrow 1} C = \underbrace{2^{4V} \cdot 2^{7V/2}}_{2^{15V/2}} \cdot \text{Diagram} \quad (\text{A.9})$$

Applying the generalized bialgebra GB along the curved wires, along with spider fusions SF, we get

$$D_{p \leftarrow 1} C = \underbrace{2^{15V/2} \cdot 2^{9V/2}}_{2^{12V}} \cdot \text{Diagram} \quad (\text{A.10})$$

After a series of spider fusions SF and color changes CC', we can modify the above diagram to

$$D_{p \leftarrow 1} C = 2^{12V} \cdot \text{Diagram} \quad (\text{A.11})$$

We now apply the generalized bialgebra GB again to get

$$D_{p \leftarrow 1} C = \frac{2^{12V}}{2^{9V/2}} \underbrace{2^{15V/2}}_{2^{15V/2}} \cdot \text{Diagram} \quad (\text{A.12})$$

Using state copy SC, spider fusion SF, and color change CC', we finally get

$$D_{p \leftarrow 1} C = \frac{2^{15V/2}}{2^{3V/2}} \underbrace{2^{6V}}_{2^{6V}} \cdot \text{Diagram} = \langle + \cdots + | C | + \cdots + \rangle D_{p \leftarrow 1}, \quad (\text{A.13})$$

where, up to scalar factors, we identified the left diagram as the operator $D_{p \leftarrow 1}$ and the right diagram as the matrix element $\langle + \cdots + | C | + \cdots + \rangle$. The latter can be seen as follows:

$$\langle + \cdots + | C | + \cdots + \rangle = \frac{2^{7V/2}}{2^{3V}} \underbrace{2^{V/2}}_{2^{V/2}} \cdot \text{Diagram} \stackrel{\text{SC, SF, S}}{=} \frac{2^{V/2} \cdot 2^{3V}}{2^{3V/2}} \underbrace{2^{2V}}_{2^{2V}} \cdot \text{Diagram} \quad (\text{A.14})$$

Multiplying $T_{1 \leftarrow p}$ on the left on both sides of (A.13) gives $DC = \langle + \cdots + | C | + \cdots + \rangle D$.³⁵ The matrix

³⁵The matrix element $\langle + \cdots + | C | + \cdots + \rangle$ can be interpreted as the partition function of the 3d (classical) topological \mathbb{Z}_2 gauge theory on T^3 . This is the lattice counterpart of the continuum result in the second line of (5.33), where the fusion coefficient $(\mathcal{Z}_2)_0$ is the partition function of the 3d \mathbb{Z}_2 gauge theory.

element here can be computed using (5.26):

$$\langle + \cdots + | C | + \cdots + \rangle = \frac{1}{2} \cdot 2^3 = 4, \quad (\text{A.15})$$

from which, we get $DC = 4D$. Similarly, one finds $CD = 4D$.

A.3 Action of D on the states

Below we derive the action of D in (5.41) using ZX-calculus. First, using (5.6), we have

$$D|\xi\rangle = 2^{(V-1)/2} D|0 \cdots 0\rangle. \quad (\text{A.16})$$

Now, we have

$$D_{p \leftarrow 1} |0 \cdots 0\rangle = \underbrace{\frac{2^{4V}}{2^{9V/2}}}_{1/2^{V/2}} \cdot \text{Diagram} \quad (\text{A.17})$$

Applying state copy SC through green dots on the links, color change CC', and spider fusion SF into the green dots on the plaquettes, we get

$$D_{p \leftarrow 1} |0 \cdots 0\rangle = \frac{1}{2^{V/2} \cdot 2^{9V/2}} \cdot \text{Diagram} \quad (\text{A.18})$$

Multiplying by $T_{1 \leftarrow p}$ on the left on both sides, we get

$$D|0 \cdots 0\rangle = \frac{1}{2^{V/2}} |+\cdots+\rangle \implies D|\xi\rangle = \frac{1}{\sqrt{2}} |+\cdots+\rangle. \quad (\text{A.19})$$

Using (5.20) and (5.24), we further have

$$D|+\cdots+\rangle = \sqrt{2} D^2 |\xi\rangle = \frac{1}{\sqrt{2}} \prod_{i < j} (1 + \eta_{ij}) \prod_s \left(\frac{1 + G_s}{2} \right) |\xi\rangle = \frac{1}{\sqrt{2}} \sum_{\xi \in \{0,1\}^3} |\xi\rangle. \quad (\text{A.20})$$

Hence, we have derived (5.41).

A.4 Ground states of 3+1d toric code

Here, we relate the loop-gas and membrane-gas representations of the ground states of the 3+1d toric code.

Recall that the ground states of the 3+1d toric code are given by (5.38),

$$|\xi\rangle := 2^{(V-1)/2} \prod_{i<j} \eta_{ij}^{\xi_{ij}} \prod_s \left(\frac{1+G_s}{2} \right) |0 \cdots 0\rangle, \quad (\text{A.21})$$

where $\xi = (\xi_{xy}, \xi_{yz}, \xi_{zx}) \in \{0, 1\}^3$ with ξ_{ij} defined modulo 2. An alternative basis for these states is

$$|\zeta\rangle := \frac{1}{2\sqrt{2}} \sum_{\xi \in \{0,1\}^3} (-1)^{\sum_{i<j} \zeta_{ij} \xi_{ij}} |\xi\rangle, \quad (\text{A.22})$$

where $\zeta = (\zeta_{xy}, \zeta_{yz}, \zeta_{zx}) \in \{0, 1\}^3$ with ζ_{ij} defined modulo 2.

It is instructive to write the state $|\zeta\rangle$ as

$$\begin{aligned} |\zeta\rangle &= 2 \cdot 2^{V/2} \prod_{i<j} \left(\frac{1 + (-1)^{\zeta_{ij}} \eta_{ij}}{2} \right) \prod_s \left(\frac{1+G_s}{2} \right) |0 \cdots 0\rangle \\ &= 2^{V-1} \prod_{\substack{i,j,k \\ \text{cyclic}}} W_k^{\zeta_{ij}} \prod_p \left(\frac{1 + \prod_{\ell \in p} Z_\ell}{2} \right) |+\cdots+\rangle, \end{aligned} \quad (\text{A.23})$$

where $W_k := W(\gamma_k)$ is the Wilson line operator (5.19) along the curve γ_k , which is a non-contractible cycle in the k th spatial direction.³⁶ One can recognize the first (second) line of (A.23) as the membrane-gas (loop-gas) representation of the ground states of the 3+1d toric code.

We can use ZX-calculus to quickly see the equality of these two representations. Consider the

³⁶Since W_k is multiplied by $\prod_p \left(\frac{1 + \prod_{\ell \in p} Z_\ell}{2} \right)$ in (A.23), the choice of γ_k does not matter.

state $|\zeta = 0\rangle$ for simplicity (the other states are obtained by multiplying $\prod_{\substack{i,j,k \\ \text{cyclic}}} W_k^{\zeta_{ij}}$). We have

$$\begin{aligned}
|\zeta = 0\rangle &= 2 \cdot 2^{V/2} \prod_{i<j} \left(\frac{1 + \eta_{ij}}{2} \right) \prod_s \left(\frac{1 + G_s}{2} \right) |0 \dots 0\rangle \\
&= \frac{2^{V/2}}{2} C |0 \dots 0\rangle = \frac{2^{V/2} \cdot 2^{7V/2}}{\underbrace{2 \cdot 2^{3V/2}}_{\frac{2^{5V/2}}{2}}} \cdot \text{Diagram}
\end{aligned} \tag{A.24}$$

Applying spider fusion SF, identity removal I, and spider fusion SF again, we get

$$|\zeta = 0\rangle = \frac{2^{5V/2}}{2} \cdot \text{Diagram} \tag{A.25}$$

This diagram is called the 2-form representation of the state $|\zeta = 0\rangle$ in [160]. (See also [161] for related discussion.) Using (A.1), with Z/X spiders exchanged, on all the red dots, we get

$$|\zeta = 0\rangle = 2^{V-1} \prod_p \left(\frac{1 + \prod_{\ell \in p} Z_\ell}{2} \right) |+\dots+\rangle, \tag{A.26}$$

which proves the equality of the first and second lines of (A.23). As a consequence, we also have

$$\begin{aligned}
|\xi\rangle &= 2^{(V-1)/2} \prod_{i<j} \eta_{ij}^{\xi_{ij}} \prod_s \left(\frac{1 + G_s}{2} \right) |0 \dots 0\rangle \\
&= \sqrt{2} \cdot 2^V \prod_{\substack{i,j,k \\ \text{cyclic}}} \left(\frac{1 + (-1)^{\xi_{ij}} W_k}{2} \right) \prod_p \left(\frac{1 + \prod_{\ell \in p} Z_\ell}{2} \right) |+\dots+\rangle.
\end{aligned} \tag{A.27}$$

For the sake of completeness, we note that the state $|\xi = 0\rangle$ can be represented as

$$|\xi = 0\rangle = \frac{2^V}{\sqrt{2}} \text{SF}_{\text{I}} \frac{2^V}{\sqrt{2}} \cdot \quad (\text{A.28})$$

These diagrams correspond to the first and second lines of (A.27), respectively. The first diagram is called the 1-form representation of the state $|\xi = 0\rangle$ in [160]. (See also [161] for related discussion.) On the other hand, the second diagram can be thought of as the action of the condensation operator $C^{(2)}$ for the 2-form symmetry of the 3+1d toric code on the product state $|+\cdots+\rangle$, i.e.,

$$|\xi = 0\rangle = \frac{2^V}{\sqrt{2}} C^{(2)} |+\cdots+\rangle, \quad (\text{A.29})$$

where

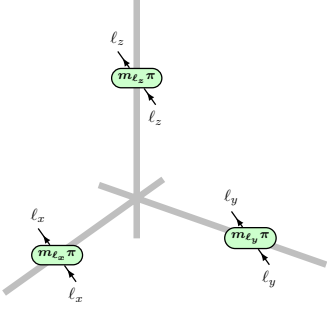
$$C^{(2)} := 2^{3V/2} \cdot \quad (\text{A.30})$$

$$= \frac{1}{2^{2V}} \sum_{\gamma} W(\gamma) = \frac{1}{4} \prod_k (1 + W_k) \prod_p \left(\frac{1 + \prod_{\ell \in p} Z_{\ell}}{2} \right).$$

B Higher quantum symmetry

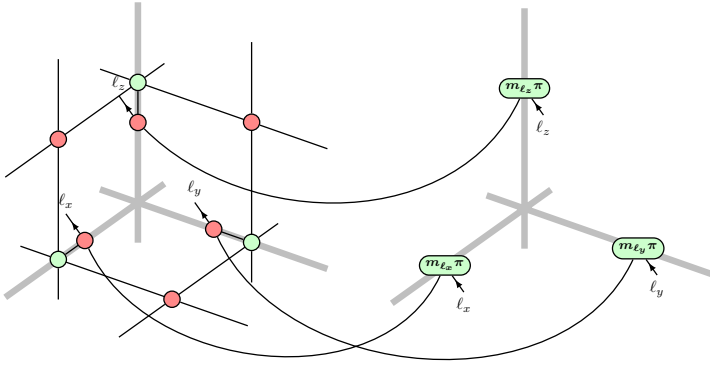
It is well-known that gauging a finite global symmetry leads to a quantum (or dual) finite symmetry [162]. For example, gauging a \mathbb{Z}_N p -form symmetry in d -dimensional spacetime gives a dual \mathbb{Z}_N $(d - p - 2)$ -form symmetry [48, 49]. Similarly, “higher gauging,” where the symmetry is gauged on a submanifold of positive codimension, results in a dual symmetry referred to as “higher quantum symmetry” [96]. One way to construct a higher quantum symmetry is by pushing a charged object from the bulk across a condensation defect. In this appendix, we use this to construct the higher quantum symmetry operators in the 3+1d lattice \mathbb{Z}_2 gauge theory.

The ZX-diagram for the Wilson line operator is

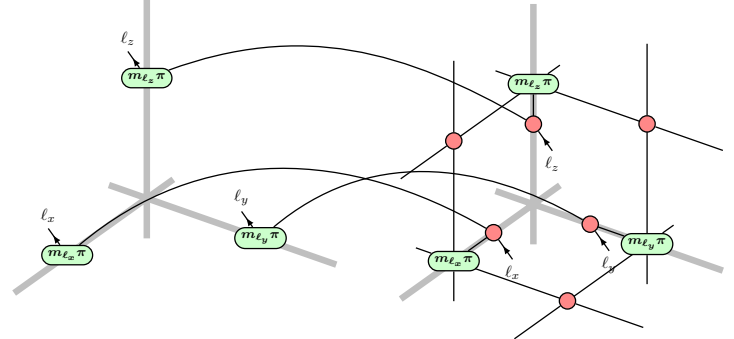
$$W(\gamma) = \prod_{\ell \in \gamma} Z_\ell = \text{Diagram} , \quad m_\ell = \delta_\gamma(\ell) , \quad (\text{B.1})$$


where γ is any (not necessarily connected) curve along the links of the lattice and $\delta_\gamma(\ell) = 1$ when $\ell \in \gamma$ and 0 otherwise, i.e., δ_γ is the indicator function for γ on the links. Recall that, when the Gauss laws are imposed exactly, $W(\gamma)$ is gauge invariant only when γ is closed. On the other hand, when the Gauss laws are imposed energetically, γ is allowed to be open and the end points of γ create Gauss law violations.

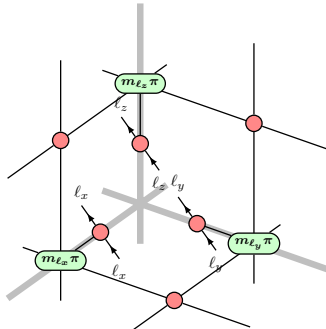
Consider the commutation of condensation operator \mathbb{C} with Wilson line operator $W(\gamma)$:

$$\mathbb{C}W(\gamma) = 2^{7V/2} \text{Diagram} , \quad m_\ell = \delta_\gamma(\ell) . \quad (\text{B.2})$$


Using π commutation Pi or identity removal I followed by spider fusion SF, we get³⁷

$$\begin{aligned}
 CW(\gamma) &= 2^{7V/2} \\
 &= W(\gamma)C(\gamma),
 \end{aligned}
 \tag{B.4}$$


where we defined

$$C(\gamma) := 2^{7V/2},
 \tag{B.5}$$


Note that a similar derivation as in Appendix A.1 gives

$$C(\gamma) = \frac{1}{2} \prod_{i < j} [1 + (-1)^{\langle \gamma, \widehat{\Sigma}_{ij} \rangle} \eta_{ij}] \prod_s \left(\frac{1 + (-1)^{\delta_{\partial\gamma}(s)} G_s}{2} \right),
 \tag{B.6}$$

where $\langle \gamma, \widehat{\Sigma}_{ij} \rangle$ is the intersection number of γ and $\widehat{\Sigma}_{ij}$, and $\delta_{\partial\gamma}(s) = 1$ when $s \in \partial\gamma$ and 0 otherwise, i.e., $\delta_{\partial\gamma}$ is the indicator function for $\partial\gamma$, the set of end points of γ .

Recall that higher gauging a \mathbb{Z}_2 1-form symmetry on a 3-dimensional submanifold gives a \mathbb{Z}_2 1-form higher quantum (or dual) symmetry on that submanifold. The operator $C(\gamma)$ is the higher

³⁷The 1+1d counterpart of this equation is

$$(1 + \eta)Z_i = 2^{L/2} \begin{array}{c} \vdots \\ \bullet \\ \vdots \\ i - \pi - i \\ \vdots \\ \bullet \\ \vdots \end{array} \stackrel{\text{Pi, SF}}{=} 2^{L/2} \begin{array}{c} \vdots \\ \pi \\ \vdots \\ i - \pi - i \\ \vdots \\ \bullet \\ \vdots \end{array} = Z_i(1 - \eta),
 \tag{B.3}$$

where $C_0 = 1 + \eta$ can be viewed as the condensation operator for an ordinary \mathbb{Z}_2 symmetry. The higher quantum symmetry is $C_1 = 1 - \eta$.

quantum symmetry operator at a fixed time slice.

The higher quantum symmetry operator $C(\gamma)$ depends only on the topology of γ . Indeed, using spider fusion SF and π commutation Pi, one can show that $C(\gamma) = C$ whenever γ is a closed contractible curve. For example, when γ is the boundary of a plaquette p , i.e., $\gamma = \partial p$, we have

$$\begin{array}{ccc}
 \begin{array}{c} \text{Diagram 1: } C(\partial p) = 2^{7V/2} \\ \text{Diagram 2: } \text{SF} \equiv 2^{7V/2} \end{array} & & \begin{array}{c} \text{Diagram 3: } \\ \text{Diagram 4: } \text{Pi} \equiv 2^{7V/2} \end{array} \\
 \begin{array}{c} \text{Diagram 5: } \text{SF} \equiv 2^{7V/2} \\ \text{Diagram 6: } \text{SF} \equiv 2^{7V/2} \end{array} & & \begin{array}{c} \text{Diagram 7: } \\ \text{Diagram 8: } \end{array} \\
 \text{Diagram 8} & & = C,
 \end{array}
 \tag{B.7}$$

where we show only a part of the ZX-diagram around the plaquette p . It follows that $C(\gamma) = C(\gamma')$ whenever γ and γ' have the same end points and $[\gamma - \gamma'] = 0 \in H_1(M, \mathbb{Z}_2)$, where M is the original lattice.

References

- [1] J. McGreevy, *Generalized Symmetries in Condensed Matter*, [arXiv:2204.03045](#).
- [2] C. Cordova, T. T. Dumitrescu, K. Intriligator, and S.-H. Shao, *Snowmass White Paper: Generalized Symmetries in Quantum Field Theory and Beyond*, in *Snowmass 2021*, 5, 2022. [arXiv:2205.09545](#).
- [3] T. D. Brennan and S. Hong, *Introduction to Generalized Global Symmetries in QFT and Particle Physics*, [arXiv:2306.00912](#).

- [4] L. Bhardwaj, L. E. Bottini, L. Fraser-Taliente, L. Gladden, D. S. W. Gould, A. Platschorre, and H. Tillim, *Lectures on generalized symmetries*, *Phys. Rept.* **1051** (2024) 1–87, [[arXiv:2307.07547](#)].
- [5] S. Schafer-Nameki, *ICTP Lectures on (Non-)Invertible Generalized Symmetries*, [arXiv:2305.18296](#).
- [6] R. Luo, Q.-R. Wang, and Y.-N. Wang, *Lecture notes on generalized symmetries and applications*, *Phys. Rept.* **1065** (2024) 1–43, [[arXiv:2307.09215](#)].
- [7] S.-H. Shao, *What’s Done Cannot Be Undone: TASI Lectures on Non-Invertible Symmetries*, [arXiv:2308.00747](#).
- [8] N. Carqueville, M. Del Zotto, and I. Runkel, *Topological defects*, 11, 2023. [arXiv:2311.02449](#).
- [9] U. Grimm and G. M. Schutz, *The Spin 1/2 XXZ Heisenberg chain, the quantum algebra $U(q)[sl(2)]$, and duality transformations for minimal models*, *J. Statist. Phys.* **71** (1993) 921–964, [[hep-th/0111083](#)].
- [10] M. Oshikawa and I. Affleck, *Boundary conformal field theory approach to the critical two-dimensional Ising model with a defect line*, *Nucl. Phys. B* **495** (1997) 533–582, [[cond-mat/9612187](#)].
- [11] W. W. Ho, L. Cincio, H. Moradi, D. Gaiotto, and G. Vidal, *Edge-entanglement spectrum correspondence in a nonchiral topological phase and Kramers-Wannier duality*, *Phys. Rev. B* **91** (2015), no. 12 125119, [[arXiv:1411.6932](#)].
- [12] M. Hauru, G. Evenbly, W. W. Ho, D. Gaiotto, and G. Vidal, *Topological conformal defects with tensor networks*, *Phys. Rev. B* **94** (2016), no. 11 115125, [[arXiv:1512.03846](#)].
- [13] D. Aasen, R. S. K. Mong, and P. Fendley, *Topological Defects on the Lattice I: The Ising model*, *J. Phys. A* **49** (2016), no. 35 354001, [[arXiv:1601.07185](#)].
- [14] N. Seiberg and S.-H. Shao, *Majorana chain and Ising model – (non-invertible) translations, anomalies, and emanant symmetries*, *SciPost Phys.* **16** (2024) 064, [[arXiv:2307.02534](#)].
- [15] N. Seiberg, S. Seifnashri, and S.-H. Shao, *Non-invertible symmetries and LSM-type constraints on a tensor product Hilbert space*, [arXiv:2401.12281](#).
- [16] A. Feiguin, S. Trebst, A. W. W. Ludwig, M. Troyer, A. Kitaev, Z. Wang, and M. H. Freedman, *Interacting anyons in topological quantum liquids: The golden chain*, *Phys. Rev. Lett.* **98** (2007) 160409, [[cond-mat/0612341](#)].
- [17] D. Aasen, P. Fendley, and R. S. K. Mong, *Topological Defects on the Lattice: Dualities and Degeneracies*, [arXiv:2008.08598](#).

- [18] M. Levin, *Constraints on order and disorder parameters in quantum spin chains*, *Commun. Math. Phys.* **378** (2020), no. 2 1081–1106, [arXiv:1903.09028].
- [19] K. Inamura, *On lattice models of gapped phases with fusion category symmetries*, *JHEP* **03** (2022) 036, [arXiv:2110.12882].
- [20] M. T. Tan, Y. Wang, and A. Mitra, *Topological Defects in Floquet Circuits*, arXiv:2206.06272.
- [21] L. Eck and P. Fendley, *From the XXZ chain to the integrable Rydberg-blockade ladder via non-invertible duality defects*, arXiv:2302.14081.
- [22] A. Mitra, H.-C. Yeh, F. Yan, and A. Rosch, *Nonintegrable Floquet Ising model with duality twisted boundary conditions*, *Phys. Rev. B* **107** (2023), no. 24 245416, [arXiv:2304.05488].
- [23] M. Sinha, F. Yan, L. Grans-Samuelsson, A. Roy, and H. Saleur, *Lattice Realizations of Topological Defects in the critical (1+1)-d Three-State Potts Model*, arXiv:2310.19703.
- [24] C. Fechisin, N. Tantivasadakarn, and V. V. Albert, *Non-invertible symmetry-protected topological order in a group-based cluster state*, arXiv:2312.09272.
- [25] H. Yan and L. Li, *Generalized Kramers-Wannier Duality from Bilinear Phase Map*, arXiv:2403.16017.
- [26] M. Okada and Y. Tachikawa, *Non-invertible symmetries act locally by quantum operations*, arXiv:2403.20062.
- [27] S. Seifnashri and S.-H. Shao, *Cluster state as a non-invertible symmetry protected topological phase*, arXiv:2404.01369.
- [28] L. Bhardwaj, L. E. Bottini, S. Schafer-Nameki, and A. Tiwari, *Illustrating the Categorical Landau Paradigm in Lattice Models*, arXiv:2405.05302.
- [29] A. Chatterjee, O. M. Aksoy, and X.-G. Wen, *Quantum Phases and Transitions in Spin Chains with Non-Invertible Symmetries*, arXiv:2405.05331.
- [30] L. Bhardwaj, L. E. Bottini, S. Schafer-Nameki, and A. Tiwari, *Lattice Models for Phases and Transitions with Non-Invertible Symmetries*, arXiv:2405.05964.
- [31] M. Khan, S. A. B. Z. Khan, and A. Mohd, *Quantum operations for Kramers-Wannier duality*, arXiv:2405.09361.
- [32] Z. Jia, *Generalized cluster states from Hopf algebras: non-invertible symmetry and Hopf tensor network representation*, arXiv:2405.09277.
- [33] D.-C. Lu, Z. Sun, and Y.-Z. You, *Realizing triality and p-ality by lattice twisted gauging in (1+1)d quantum spin systems*, arXiv:2405.14939.

- [34] Y. Li and M. Litvinov, *Non-invertible SPT, gauging and symmetry fractionalization*, [arXiv:2405.15951](#).
- [35] T. Ando, *A journey on self-G-ality*, [arXiv:2405.15648](#).
- [36] N. O’Dea, *Level statistics detect generalized symmetries*, [arXiv:2406.03983](#).
- [37] C. Delcamp and A. Tiwari, *Higher categorical symmetries and gauging in two-dimensional spin systems*, *SciPost Phys.* **16** (2024) 110, [[arXiv:2301.01259](#)].
- [38] K. Inamura and K. Ohmori, *Fusion Surface Models: 2+1d Lattice Models from Fusion 2-Categories*, [arXiv:2305.05774](#).
- [39] H. Moradi, O. M. Aksoy, J. H. Bardarson, and A. Tiwari, *Symmetry fractionalization, mixed-anomalies and dualities in quantum spin models with generalized symmetries*, [arXiv:2307.01266](#).
- [40] W. Cao, L. Li, M. Yamazaki, and Y. Zheng, *Subsystem Non-Invertible Symmetry Operators and Defects*, [arXiv:2304.09886](#).
- [41] W. Cao and Q. Jia, *Symmetry TFT for Subsystem Symmetry*, [arXiv:2310.01474](#).
- [42] A. Parayil Mana, Y. Li, H. Sukeno, and T.-C. Wei, *Kennedy-Tasaki transformation and non-invertible symmetry in lattice models beyond one dimension*, [arXiv:2402.09520](#).
- [43] R. C. Spieler, *Non-Invertible Duality Interfaces in Field Theories with Exotic Symmetries*, [arXiv:2402.14944](#).
- [44] Y. Choi, Y. Sanghavi, S.-H. Shao, and Y. Zheng, *Non-invertible and higher-form symmetries in 2+1d lattice gauge theories*, [arXiv:2405.13105](#).
- [45] P.-S. Hsin, R. Kobayashi, and C. Zhang, *Fractionalization of Coset Non-Invertible Symmetry and Exotic Hall Conductance*, [arXiv:2405.20401](#).
- [46] W. Cao, L. Li, and M. Yamazaki, *Generating Lattice Non-invertible Symmetries*, [arXiv:2406.05454](#).
- [47] F. J. Wegner, *Duality in Generalized Ising Models and Phase Transitions Without Local Order Parameters*, *J. Math. Phys.* **12** (1971) 2259–2272.
- [48] D. Gaiotto, A. Kapustin, N. Seiberg, and B. Willett, *Generalized Global Symmetries*, *JHEP* **02** (2015) 172, [[arXiv:1412.5148](#)].
- [49] Y. Tachikawa, *On gauging finite subgroups*, *SciPost Phys.* **8** (2020), no. 1 015, [[arXiv:1712.09542](#)].
- [50] M. Koide, Y. Nagoya, and S. Yamaguchi, *Non-invertible topological defects in 4-dimensional \mathbb{Z}_2 pure lattice gauge theory*, *PTEP* **2022** (2022), no. 1 013B03, [[arXiv:2109.05992](#)].

- [51] Y. Choi, C. Cordova, P.-S. Hsin, H. T. Lam, and S.-H. Shao, *Noninvertible duality defects in 3+1 dimensions*, *Phys. Rev. D* **105** (2022), no. 12 125016, [arXiv:2111.01139].
- [52] J. Kaidi, K. Ohmori, and Y. Zheng, *Kramers-Wannier-like Duality Defects in (3+1)D Gauge Theories*, *Phys. Rev. Lett.* **128** (2022), no. 11 111601, [arXiv:2111.01141].
- [53] R. Orús, *Tensor networks for complex quantum systems*, *APS Physics* **1** (2019) 538–550, [arXiv:1812.04011].
- [54] J. I. Cirac, D. Perez-Garcia, N. Schuch, and F. Verstraete, *Matrix product states and projected entangled pair states: Concepts, symmetries, theorems*, *Rev. Mod. Phys.* **93** (2021), no. 4 045003, [arXiv:2011.12127].
- [55] F. Verstraete, J. J. García-Ripoll, and J. I. Cirac, *Matrix Product Density Operators: Simulation of Finite-Temperature and Dissipative Systems*, *Phys. Rev. Lett.* **93** (2004), no. 20 207204, [arXiv/cond-mat/0406440].
- [56] M. Zwolak and G. Vidal, *Mixed-State Dynamics in One-Dimensional Quantum Lattice Systems: A Time-Dependent Superoperator Renormalization Algorithm*, *Phys. Rev. Lett.* **93** (2004), no. 20 207205, [arXiv/cond-mat/0406426].
- [57] N. Bultinck, M. Mariën, D. J. Williamson, M. B. Şahinoğlu, J. Haegeman, and F. Verstraete, *Anyons and matrix product operator algebras*, *Annals Phys.* **378** (2017) 183–233, [arXiv:1511.08090].
- [58] R. Vanhove, M. Bal, D. J. Williamson, N. Bultinck, J. Haegeman, and F. Verstraete, *Mapping topological to conformal field theories through strange correlators*, *Phys. Rev. Lett.* **121** (2018), no. 17 177203, [arXiv:1801.05959].
- [59] L. Lootens, C. Delcamp, G. Ortiz, and F. Verstraete, *Dualities in One-Dimensional Quantum Lattice Models: Symmetric Hamiltonians and Matrix Product Operator Intertwiners*, *PRX Quantum* **4** (2023), no. 2 020357, [arXiv:2112.09091].
- [60] J. Garre-Rubio, L. Lootens, and A. Molnár, *Classifying phases protected by matrix product operator symmetries using matrix product states*, *Quantum* **7** (2023) 927, [arXiv:2203.12563].
- [61] A. Molnar, A. R. de Alarcón, J. Garre-Rubio, N. Schuch, J. I. Cirac, and D. Pérez-García, *Matrix product operator algebras I: representations of weak Hopf algebras and projected entangled pair states*, arXiv:2204.05940.
- [62] A. Ruiz-de Alarcón, J. Garre-Rubio, A. Molnár, and D. Pérez-García, *Matrix Product Operator Algebras II: Phases of Matter for 1D Mixed States*, arXiv:2204.06295.
- [63] L. Lootens, C. Delcamp, and F. Verstraete, *Dualities in One-Dimensional Quantum Lattice Models: Topological Sectors*, *PRX Quantum* **5** (2024), no. 1 010338, [arXiv:2211.03777].

- [64] L. Lootens, C. Delcamp, D. Williamson, and F. Verstraete, *Low-depth unitary quantum circuits for dualities in one-dimensional quantum lattice models*, [arXiv:2311.01439](#).
- [65] B. Coecke and R. Duncan, *Interacting Quantum Observables*, *Lect. Notes Comput. Sci.* **5126** (2008) 298–310.
- [66] R. Duncan and B. Coecke, *Interacting quantum observables: categorical algebra and diagrammatics*, *New J. Phys.* **13** (2011), no. 4 043016, [[arXiv:0906.4725](#)].
- [67] J. van de Wetering, *ZX-calculus for the working quantum computer scientist*, [arXiv:2012.13966](#).
- [68] P. Selinger, *A Survey of Graphical Languages for Monoidal Categories*, pp. 289–355. Springer Berlin Heidelberg, 2010. [arXiv:0908.3347](#).
- [69] B. Coecke and A. Kissinger, *Picturing Quantum Processes: A First Course in Quantum Theory and Diagrammatic Reasoning*. Cambridge University Press, 2017.
- [70] A. Kissinger and J. van de Wetering, *Reducing the number of non-Clifford gates in quantum circuits*, *Phys. Rev. A* **102** (2020), no. 2 022406, [[arXiv:1903.10477](#)].
- [71] N. de Beaudrap, X. Bian, and Q. Wang, *Techniques to reduce $\pi/4$ -parity-phase circuits, motivated by the zx calculus*, *Electronic Proceedings in Theoretical Computer Science* **318** (May, 2020) 131–149, [[arXiv:1911.09039](#)].
- [72] N. de Beaudrap, X. Bian, and Q. Wang, *Fast and Effective Techniques for T-Count Reduction via Spider Nest Identities*, *Leibniz Int. Proc. Inf.* **158** (2020) 11:1–11:23, [[arXiv:2004.05164](#)].
- [73] N. de Beaudrap and D. Horsman, *The zx calculus is a language for surface code lattice surgery*, *Quantum* **4** (Jan., 2020) 218, [[arXiv:1704.08670](#)].
- [74] A. Kissinger, *Phase-free ZX diagrams are CSS codes (...or how to graphically grok the surface code)*, [arXiv:2204.14038](#).
- [75] A. B. Khesin, J. Z. Lu, and P. W. Shor, *Graphical quantum Clifford-encoder compilers from the ZX calculus*, [arXiv:2301.02356](#).
- [76] H. Bombin, D. Litinski, N. Nickerson, F. Pastawski, and S. Roberts, *Unifying flavors of fault tolerance with the ZX calculus*, [arXiv:2303.08829](#).
- [77] A. Bauer, *Topological error correcting processes from fixed-point path integrals*, *Quantum* **8** (2024) 1288, [[arXiv:2303.16405](#)].
- [78] H. Bombin, C. Dawson, T. Farrelly, Y. Liu, N. Nickerson, M. Pant, F. Pastawski, and S. Roberts, *Fault-tolerant complexes*, [arXiv:2308.07844](#).

- [79] A. Townsend-Teague, J. M. de la Fuente, and M. Kesselring, *Floquetifying the Colour Code*, *EPTCS* **384** (2023) 265–303, [arXiv:2307.11136].
- [80] E. O’Brien and P. Fendley, *Lattice supersymmetry and order-disorder coexistence in the tricritical Ising model*, *Phys. Rev. Lett.* **120** (2018), no. 20 206403, [arXiv:1712.06662].
- [81] X. Chen, A. Dua, M. Hermele, D. T. Stephen, N. Tantivasadakarn, R. Vanhove, and J.-Y. Zhao, *Sequential Quantum Circuits as Maps between Gapped Phases*, arXiv:2307.01267.
- [82] N. Tantivasadakarn, R. Thorngren, A. Vishwanath, and R. Verresen, *Long-Range Entanglement from Measuring Symmetry-Protected Topological Phases*, *Phys. Rev. X* **14** (2024), no. 2 021040, [arXiv:2112.01519].
- [83] L. Li, M. Oshikawa, and Y. Zheng, *Noninvertible duality transformation between symmetry-protected topological and spontaneous symmetry breaking phases*, *Phys. Rev. B* **108** (2023), no. 21 214429, [arXiv:2301.07899].
- [84] N. Tantivasadakarn, A. Vishwanath, and R. Verresen, *Hierarchy of Topological Order From Finite-Depth Unitaries, Measurement, and Feedforward*, *PRX Quantum* **4** (2023), no. 2 020339, [arXiv:2209.06202].
- [85] P. Pfeuty, *The one-dimensional Ising model with a transverse field*, *Annals Phys.* **57** (1970), no. 1 79–90.
- [86] P. Gorantla, H. T. Lam, N. Seiberg, and S.-H. Shao, *A modified Villain formulation of fractons and other exotic theories*, *J. Math. Phys.* **62** (2021), no. 10 102301, [arXiv:2103.01257].
- [87] N. Seiberg, *Field Theories With a Vector Global Symmetry*, *SciPost Phys.* **8** (2020), no. 4 050, [arXiv:1909.10544].
- [88] M. Qi, L. Radzihovsky, and M. Hermele, *Fracton phases via exotic higher-form symmetry-breaking*, *Annals Phys.* **424** (2021) 168360, [arXiv:2010.02254].
- [89] X.-G. Wen, *Emergent anomalous higher symmetries from topological order and from dynamical electromagnetic field in condensed matter systems*, *Phys. Rev. B* **99** (2019), no. 20 205139, [arXiv:1812.02517].
- [90] Y.-A. Chen, T. D. Ellison, and N. Tantivasadakarn, *Disentangling supercohomology symmetry-protected topological phases in three spatial dimensions*, *Phys. Rev. Res.* **3** (2021), no. 1 013056, [arXiv:2008.05652].
- [91] M. Levin and Z.-C. Gu, *Braiding statistics approach to symmetry-protected topological phases*, *Phys. Rev. B* **86** (2012) 115109, [arXiv:1202.3120].
- [92] B. Yoshida, *Topological phases with generalized global symmetries*, *Phys. Rev. B* **93** (2016), no. 15 155131, [arXiv:1508.03468].

- [93] P.-S. Hsin and C. Zhang, *Kramers-Wannier Dualities and Quantum Cellular Automata*, to appear.
- [94] Y. Choi, H. T. Lam, and S.-H. Shao, *Noninvertible Global Symmetries in the Standard Model*, *Phys. Rev. Lett.* **129** (2022), no. 16 161601, [[arXiv:2205.05086](#)].
- [95] Y. Choi, C. Cordova, P.-S. Hsin, H. T. Lam, and S.-H. Shao, *Non-invertible Condensation, Duality, and Triality Defects in 3+1 Dimensions*, *Commun. Math. Phys.* **402** (2023), no. 1 489–542, [[arXiv:2204.09025](#)].
- [96] K. Roumpedakis, S. Seifnashri, and S.-H. Shao, *Higher Gauging and Non-invertible Condensation Defects*, *Commun. Math. Phys.* **401** (2023), no. 3 3043–3107, [[arXiv:2204.02407](#)].
- [97] M. Creutz, L. Jacobs, and C. Rebbi, *Monte carlo study of abelian lattice gauge theories*, *Phys. Rev. D* **20** (Oct, 1979) 1915–1922.
- [98] E. Lieb, T. Schultz, and D. Mattis, *Two soluble models of an antiferromagnetic chain*, *Annals of Physics* **16** (1961) 407.
- [99] C.-M. Chang, Y.-H. Lin, S.-H. Shao, Y. Wang, and X. Yin, *Topological Defect Lines and Renormalization Group Flows in Two Dimensions*, *JHEP* **01** (2019) 026, [[arXiv:1802.04445](#)].
- [100] R. Thorngren and Y. Wang, *Fusion Category Symmetry I: Anomaly In-Flow and Gapped Phases*, [arXiv:1912.02817](#).
- [101] Y. Choi, H. T. Lam, and S.-H. Shao, *Noninvertible Time-Reversal Symmetry*, *Phys. Rev. Lett.* **130** (2023), no. 13 131602, [[arXiv:2208.04331](#)].
- [102] J. Kaidi, E. Nardoni, G. Zafrir, and Y. Zheng, *Symmetry TFTs and anomalies of non-invertible symmetries*, *JHEP* **10** (2023) 053, [[arXiv:2301.07112](#)].
- [103] C. Zhang and C. Córdova, *Anomalies of $(1+1)D$ categorical symmetries*, [arXiv:2304.01262](#).
- [104] C. Cordova, P.-S. Hsin, and C. Zhang, *Anomalies of Non-Invertible Symmetries in $(3+1)d$* , [arXiv:2308.11706](#).
- [105] A. Antinucci, F. Benini, C. Copetti, G. Galati, and G. Rizi, *Anomalies of non-invertible self-duality symmetries: fractionalization and gauging*, [arXiv:2308.11707](#).
- [106] Z. Komargodski, K. Ohmori, K. Roumpedakis, and S. Seifnashri, *Symmetries and strings of adjoint QCD_2* , *JHEP* **03** (2021) 103, [[arXiv:2008.07567](#)].
- [107] Y. Choi, B. C. Rayhaun, Y. Sanghavi, and S.-H. Shao, *Remarks on boundaries, anomalies, and noninvertible symmetries*, *Phys. Rev. D* **108** (2023), no. 12 125005, [[arXiv:2305.09713](#)].

- [108] Y. Choi, D.-C. Lu, and Z. Sun, *Self-duality under gauging a non-invertible symmetry*, [arXiv:2310.19867](#).
- [109] P. Gorantla and T.-C. Huang, *to appear*.
- [110] A. Kapustin and R. Thorngren, *Higher symmetry and gapped phases of gauge theories*, [arXiv:1309.4721](#).
- [111] A. Apte, C. Cordova, and H. T. Lam, *Obstructions to gapped phases from noninvertible symmetries*, *Phys. Rev. B* **108** (2023), no. 4 045134, [[arXiv:2212.14605](#)].
- [112] O. Aharony, N. Seiberg, and Y. Tachikawa, *Reading between the lines of four-dimensional gauge theories*, *JHEP* **08** (2013) 115, [[arXiv:1305.0318](#)].
- [113] S. Vijay, J. Haah, and L. Fu, *Fracton Topological Order, Generalized Lattice Gauge Theory and Duality*, *Phys. Rev. B* **94** (2016), no. 23 235157, [[arXiv:1603.04442](#)].
- [114] D. J. Williamson, *Fractal symmetries: Ungauging the cubic code*, *Phys. Rev. B* **94** (2016), no. 15 155128, [[arXiv:1603.05182](#)].
- [115] W. Shirley, K. Slagle, and X. Chen, *Foliated fracton order from gauging subsystem symmetries*, *SciPost Phys.* **6** (2019), no. 4 041, [[arXiv:1806.08679](#)].
- [116] N. Tantivasadakarn, *Jordan-Wigner Dualities for Translation-Invariant Hamiltonians in Any Dimension: Emergent Fermions in Fracton Topological Order*, *Phys. Rev. Res.* **2** (2020), no. 2 023353, [[arXiv:2002.11345](#)].
- [117] N. Tantivasadakarn, R. Thorngren, A. Vishwanath, and R. Verresen, *Pivot Hamiltonians as generators of symmetry and entanglement*, *SciPost Phys.* **14** (2023), no. 2 012, [[arXiv:2110.07599](#)].
- [118] S. Liu and W. Ji, *Towards non-invertible anomalies from generalized Ising models*, *SciPost Phys.* **15** (2023), no. 4 150, [[arXiv:2208.09101](#)].
- [119] T. Rakovszky and V. Khemani, *The Physics of (good) LDPC Codes I. Gauging and dualities*, [arXiv:2310.16032](#).
- [120] T. Rakovszky and V. Khemani, *The Physics of (good) LDPC Codes II. Product constructions*, [arXiv:2402.16831](#).
- [121] T. Okuda, A. Parayil Mana, and H. Sukeno, *Anomaly inflow for CSS and fractonic lattice models and dualities via cluster state measurement*, [arXiv:2405.15853](#).
- [122] E. Cobanera, G. Ortiz, and Z. Nussinov, *The Bond-Algebraic Approach to Dualities*, *Adv. Phys.* **60** (2011) 679–798, [[arXiv:1103.2776](#)].

- [123] J. Haegeman, K. Van Acoleyen, N. Schuch, J. I. Cirac, and F. Verstraete, *Gauging quantum states: from global to local symmetries in many-body systems*, *Phys. Rev. X* **5** (2015), no. 1 011024, [arXiv:1407.1025].
- [124] B. Yoshida, *Gapped boundaries, group cohomology and fault-tolerant logical gates*, *Annals Phys.* **377** (2017) 387–413, [arXiv:1509.03626].
- [125] D. J. Williamson, N. Bultinck, and F. Verstraete, *Symmetry-enriched topological order in tensor networks: Defects, gauging and anyon condensation*, arXiv:1711.07982.
- [126] A. Kubica and B. Yoshida, *Ungauging quantum error-correcting codes*, arXiv:1805.01836.
- [127] D. Radičević, *Systematic Constructions of Fracton Theories*, arXiv:1910.06336.
- [128] N. Tantivasadakarn and S. Vijay, *Searching for fracton orders via symmetry defect condensation*, *Phys. Rev. B* **101** (2020), no. 16 165143, [arXiv:1912.02826].
- [129] K. Dolev, V. Calvera, S. S. Cree, and D. J. Williamson, *Gauging the bulk: generalized gauging maps and holographic codes*, *JHEP* **05** (2022) 158, [arXiv:2108.11402].
- [130] B. C. Rayhaun and D. J. Williamson, *Higher-form subsystem symmetry breaking: Subdimensional criticality and fracton phase transitions*, *SciPost Phys.* **15** (2023), no. 1 017, [arXiv:2112.12735].
- [131] R. A. Brualdi, F. Harary, and Z. Miller, *Bigraphs versus digraphs via matrices*, *Journal of Graph Theory* **4** (1980), no. 1 51–73.
- [132] J. Ashkin and E. Teller, *Statistics of two-dimensional lattices with four components*, *Phys. Rev.* **64** (Sep, 1943) 178–184.
- [133] C. Fan, *On critical properties of the ashkin-teller model*, *Physics Letters A* **39** (1972), no. 2 136.
- [134] J. Sólyom, *Duality of the block transformation and decimation for quantum spin systems*, *Phys. Rev. B* **24** (Jul, 1981) 230–243.
- [135] M. Kohmoto, M. den Nijs, and L. P. Kadanoff, *Hamiltonian studies of the $d = 2$ ashkin-teller model*, *Phys. Rev. B* **24** (Nov, 1981) 5229–5241.
- [136] H. Saleur, *Partition functions of the two-dimensional ashkin-teller model on the critical line*, *Journal of Physics A: Mathematical and General* **20** (nov, 1987) L1127.
- [137] P. Gorantla, H. T. Lam, N. Seiberg, and S.-H. Shao, *Global dipole symmetry, compact Lifshitz theory, tensor gauge theory, and fractons*, *Phys. Rev. B* **106** (2022), no. 4 045112, [arXiv:2201.10589].
- [138] S. D. Pace, G. Delfino, H. T. Lam, and O. M. Aksoy, *Gauging modulated symmetries: Kramers-Wannier dualities and non-invertible reflections*, to appear.

- [139] J. C. Bridgeman, A. O’Brien, S. D. Bartlett, and A. C. Doherty, *Multiscale entanglement renormalization ansatz for spin chains with continuously varying criticality*, *Phys. Rev. B* **91** (2015), no. 16 165129, [arXiv:1501.02817].
- [140] J. C. Bridgeman and D. J. Williamson, *Anomalies and entanglement renormalization*, *Phys. Rev. B* **96** (2017), no. 12 125104, [arXiv:1703.07782].
- [141] R. Thorngren and Y. Wang, *Fusion Category Symmetry II: Categoriosities at $c = 1$ and Beyond*, arXiv:2106.12577.
- [142] O. Diatlyk, C. Luo, Y. Wang, and Q. Weller, *Gauging Non-Invertible Symmetries: Topological Interfaces and Generalized Orbifold Groupoid in 2d QFT*, arXiv:2311.17044.
- [143] A. Perez-Lona, D. Robbins, E. Sharpe, T. Vandermeulen, and X. Yu, *Notes on gauging noninvertible symmetries, part 1: Multiplicity-free cases*, arXiv:2311.16230.
- [144] L. Turban, *Self-dual ising chain in a transverse field with multispin interactions*, *Journal of Physics C: Solid State Physics* **15** (feb, 1982) L65.
- [145] A. Maritan, A. Stella, and C. Vanderzande, *First- and second-order phase transitions in a system with multispin interactions*, *Phys. Rev. B* **29** (Jan, 1984) 519–521.
- [146] K. A. Penson, R. Jullien, and P. Pfeuty, *Phase transitions in systems with multispin interactions*, *Phys. Rev. B* **26** (Dec, 1982) 6334–6337.
- [147] M. Kolb and K. A. Penson, *Conformal invariance and the phase transition of a spin chain with three-spin interaction*, *Journal of Physics A: Mathematical and General* **19** (sep, 1986) L779.
- [148] F. Igloi, D. V. Kapor, M. Skrinjar, and J. Solyom, *Series expansion study of first- and second-order phase transitions in a model with multispin coupling*, *Journal of Physics A: Mathematical and General* **19** (may, 1986) 1189.
- [149] F. C. Alcaraz and M. N. Barber, *Conformal invariance and the critical behaviour of a quantum spin hamiltonian with three-spin coupling*, *Journal of Physics A: Mathematical and General* **20** (jan, 1987) 179.
- [150] A. Udupa, S. Sur, S. Nandy, A. Sen, and D. Sen, *Weak universality, quantum many-body scars, and anomalous infinite-temperature autocorrelations in a one-dimensional spin model with duality*, *Phys. Rev. B* **108** (2023), no. 21 214430, [arXiv:2307.11161].
- [151] G. Abay-Asmerom, R. H. Hammack, C. E. Larson, and D. T. Taylor, *Direct product factorization of bipartite graphs with bipartition-reversing involutions*, *SIAM J. Discret. Math.* **23** (jan, 2010) 2042–2052.
- [152] W. Cui, B. Haghighat, and L. Ruggeri, *Non-Invertible Surface Defects in 2+1d QFTs from Half Spacetime Gauging*, arXiv:2406.09261.

- [153] Q. Wang and X. Bian, *Qutrit dichromatic calculus and its universality*, *Electronic Proceedings in Theoretical Computer Science* **172** (Dec., 2014) 92–101, [[arXiv:1406.3056](#)].
- [154] Q. Wang, *Qufinite ZX-calculus: a unified framework of qudit ZX-calculi*, [arXiv:2104.06429](#).
- [155] B. Poór, R. A. Shaikh, and Q. Wang, *ZX-calculus is Complete for Finite-Dimensional Hilbert Spaces*, [arXiv:2405.10896](#).
- [156] M. Cheng and N. Seiberg, *Lieb-Schultz-Mattis, Luttinger, and 't Hooft - anomaly matching in lattice systems*, *SciPost Phys.* **15** (2023), no. 2 051, [[arXiv:2211.12543](#)].
- [157] S. Seifnashri, *Lieb-Schultz-Mattis anomalies as obstructions to gauging (non-on-site) symmetries*, [arXiv:2308.05151](#).
- [158] T. Kennedy and H. Tasaki, *Hidden symmetry breaking and the haldane phase in $s=1$ quantum spin chains*, *Communications in mathematical physics* **147** (1992) 431–484.
- [159] T. Kennedy and H. Tasaki, *Hidden $z_2 \times z_2$ symmetry breaking in haldane-gap antiferromagnets*, *Phys. Rev. B* **45** (Jan, 1992) 304–307.
- [160] D. J. Williamson, C. Delcamp, F. Verstraete, and N. Schuch, *On the stability of topological order in tensor network states*, *Phys. Rev. B* **104** (2021), no. 23 235151, [[arXiv:2012.15346](#)].
- [161] C. Delcamp and N. Schuch, *On tensor network representations of the $(3+1)d$ toric code*, *Quantum* **5** (2021) 604, [[arXiv:2012.15631](#)].
- [162] C. Vafa, *Quantum Symmetries of String Vacua*, *Mod. Phys. Lett. A* **4** (1989) 1615.